SUPPLEMENTARY INFORMATION

Identification of a systemic lupus erythematosus risk locus spanning *ATG16L2, FCHSD2,* and *P2RY2* in Koreans

Christopher J. Lessard[1, 25], Satria Sajuthi [2, 25], Jian Zhao[3, 25], Kwangwoo Kim[4, 25], John A. Ice[1], He Li[1,5], Hannah Ainsworth[2], Astrid Rasmussen[1], Jennifer A. Kelly[1], Mindy Marion[2],'So-Young Bang[4], Young Bin Joo[4], Jeongim Choi[4], Hye-Soon Lee[4], Young Mo Kang[6], Chang-Hee Suh[7], Won Tae Chung[8], Soo-Kon Lee[9], Jung-Yoon Choe[10], Seung Cheol Shim[11], Ji Hee Oh[12], Young Jin Kim[12], Bok-Ghee Han[12], Nan Shen[13,14], Hwee Siew Howe[15], Edward K. Wakeland[16], Quan-Zhen Li[16], Yeong Wook Song[17], Patrick M. Gaffney[1], Marta E. Alarcón-Riquelme [1,18], Lindsey A. Criswell[19], Chaim O. Jacob[20], Robert P. Kimberly[21], Timothy J. Vyse[22], John B. Harley[23, 24], Kathy L. Sivils[1, 4, 26], Sang-Cheol Bae[4, 26], Carl D. Langefeld[2, 26], and Betty P. Tsao[3, 26, 27]

Please note that citations may be found within the main text.

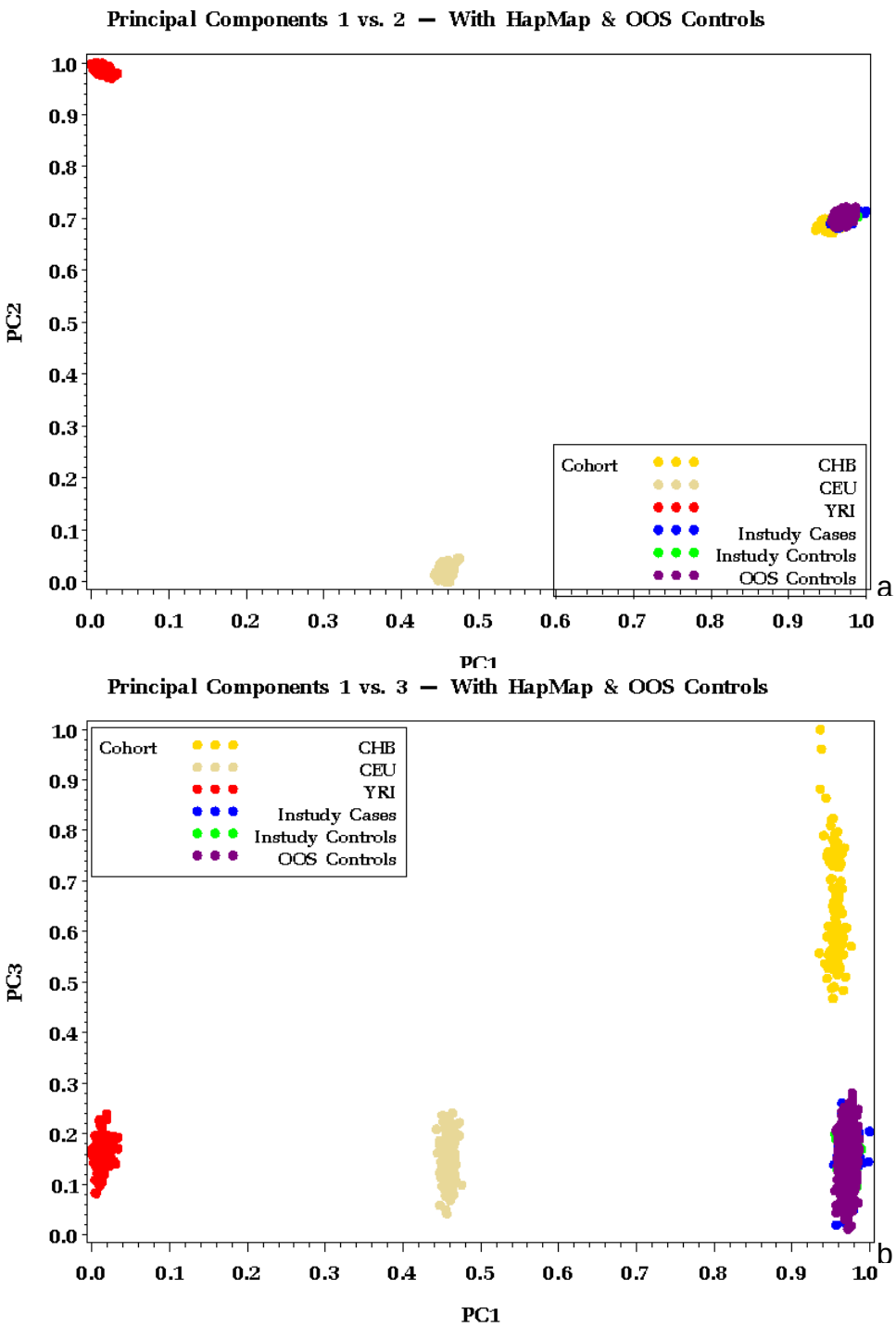

Supplementary Figure 1: Plots of the principal component analysis (PCA) for the GWA phase. PCA was performed using three HapMap populations along with the in-study cases and controls as well as out-of-study controls according to the legends. Panel (a) is a plot of PC1 (X-axis) vs PC2 (Y-axis) showing that the in-study and out-of-study samples cluster with each other and the CHB HapMap population. However, when plotting PC1 (X-axis) vs PC3 (Y-axis) in panel (b), the in-study and out-of-study samples map to the same cluster, but form a distinct population from that of the CHB HapMap subjects. In these data, PC3 defines the Korean population from the Han Chinese.

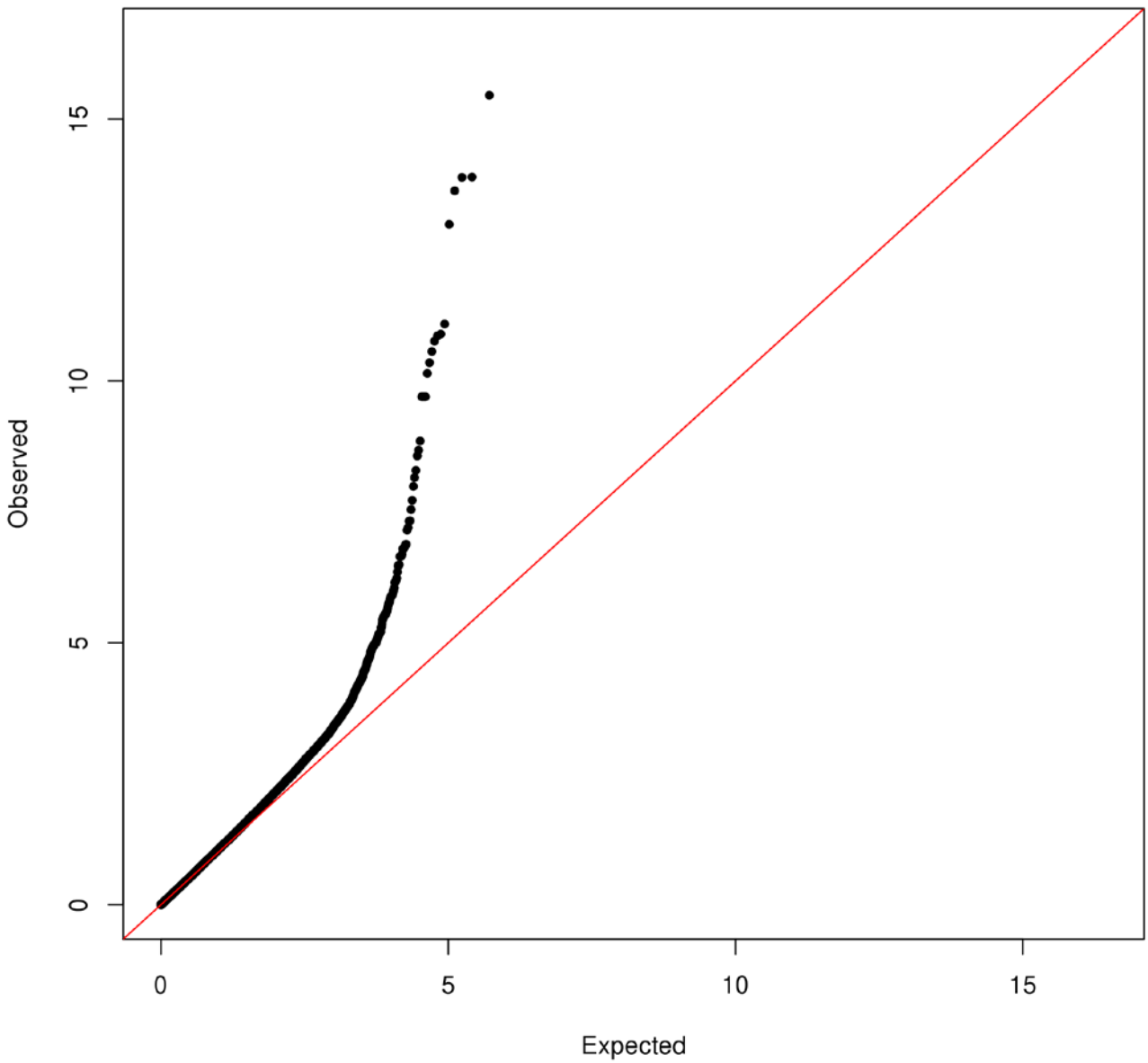

Supplementary Figure 2: Probability-probability plot of GWA scan dataset. Deviation of the $-\log_{10}$(p-value) of the expected (red line) towards observed (y-axis) was observed, but only a modest inflation was observed with $\lambda = 1.09$.

Supplementary Table 1: Summary of replication samples and case control minor allele frequencies from tested SNPs.

					rs2267828		rs10901656		rs11235667		rs1048257	
Phase	**Country of Origin**	**Location of typing**	**SLE cases**	**Controls**	**CASE**	**CTRL**	**CASE**	**CTRL**	**CASE**	**CTRL**	**CASE**	**CTRL**
Replication	Chinese	UCLA	677	709	0.38	0.40	0.21	0.19	0.07	0.10	0.37	0.37
Replication	Korea	UCLA	218	247	0.43	0.49	0.23	0.23	0.10	0.11	0.35	0.37
Replication	Korea	OMRF	521	189	0.41	0.42	0.27	0.24	0.07	0.09	0.32	0.38

For the following Supplementary Table, please see the accompanying Excel spreadsheet:

Supplementary Table 2: Results of single locus association with SLE in the region of *FCHSD2 and P2RY2* after imputation.

Please note: Missing genotypes have been imputed into this dataset if they were not called in the GWAS dataset

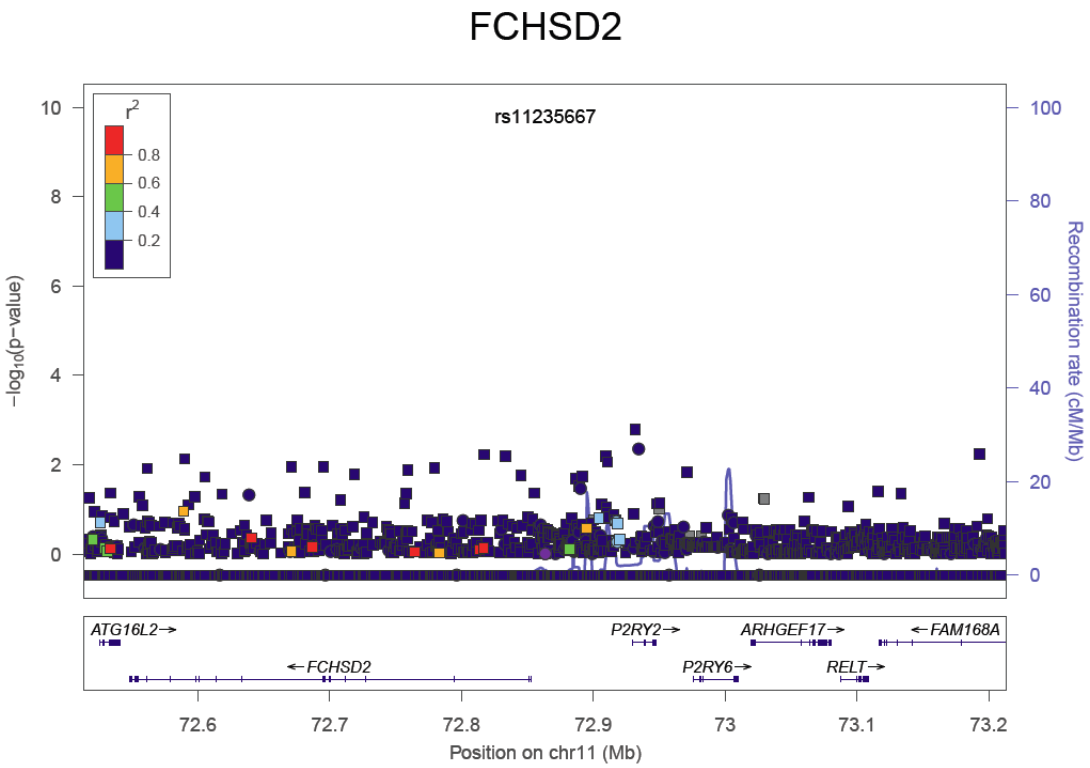

Supplementary Figure 3: Regional association plot after stepwise analysis in 11q14 region. After adding rs11235667 into the stepwise regression model, no statistically significant variant remained associated with SLE.

Supplementary Table 3: Genomic features in the region of 11q14. Note: the variant in red, rs11235667, is the most significantly associated variant in the region. This table is limited to those variants that exceeded genome-wide significance. Haploreg ver.2[13] was used as the source for these data provided by both the ENCODE[14] and Epigenetics Roadmap[15] projects.

ENCODE	
SE	Strong Enhancer
WE	Weak Enhancer
WP	Weak Promoter

ROADMAP	
WE	Weak Enhancer
AE	Active Enhancer
WTSS	Weak TSS
TxE	Transcription - Enhancer-like

Variant	Ref	Alt	DNase (ENCODE)	No. of proteins bound by ChIP (ENCODE)	No. of regulatory motifs altered	ENCODE		Roadmap																
						GM12878 (Lymphoblastoid)	K562 (Myelogenous Leukemia)	CD3 (P)	CD4 Naive (P)	CD4 Memory (P)	CD4(+) CD25(-) CD45RA(+) Naive (P)	CD4(+) CD25(-) CD45RO(+) Memory (P)	CD4(+) CD25(-) IL17(-) PMA/I stim Th (P)	CD4(+) CD25(-) IL17(+) PMA/I stim Th17 (P)	CD4(+) CD25(-) Th (P)	CD4(+) CD25int CD127(+) Tmem (P)	CD4(+) CD25(+) CD127(-) Treg (P)	CD8 Naive (P)	CD8 Memory (P)	CD15 (P)	CD19 (P)	CD34 (P)	Mobilized CD34 (P)	CD34 (C)
rs11235667	A	G	5	2	1	SE	-	AE	WE	WE	WE	-	WE	WE	AE	-	WE	WE	WE	WE	AE	AE	WE	AE
rs11235659	A	G	0	0	1	-	-	-	-	-	-	-	-	-	-	-	-	-	-	-	-	-	-	-
rs11235622	C	T	1	0	3	WE	-	-	-	-	-	-	-	-	-	-	-	-	-	-	-	AE	WE	TxE
rs77971648	T	C	0	0	4	-	-	-	-	-	-	-	-	-	-	-	-	-	-	WE	-	-	-	-
rs117527774	A	G	0	0	1	-	-	-	-	-	-	-	-	-	-	-	-	-	-	-	-	-	-	-
rs118141553	G	C	0	0	1	-	-	-	-	-	-	-	-	-	-	-	-	-	-	-	-	-	-	-
rs11235645	C	T	0	0	4	-	-	-	-	-	-	-	-	-	-	-	-	-	-	-	-	-	-	-
rs11235604	C	T	1	4	8	WP	WP	WTSS	WTSS	AE	AE	AE	AE	AE	TxE	AE	WTSS	WTSS	AE	TxE	AE	-	TxE	-
rs72981516	T	G	0	0	3	-	-	-	-	-	-	-	-	-	-	-	-	-	-	-	-	-	-	-
rs11235672	T	C	0	1	3	-	WE	-	-	-	-	-	-	-	-	-	-	-	-	-	-	-	AE	-

For the following Supplementary Table, please see the accompanying Excel spreadsheet:

Supplementary Table 4: Summary of the single locus analysis of variants in the HLA region after imputation using 1000 Genomes.

Please note: Missing genotypes have been imputed into this dataset if they were not called in the GWAS dataset

Supplementary Figure 4A: Results after stepwise analysis of the HLA region after imputation. Below are the $-\log_{10}$(P-value) for the results after each variant was added to the stepwise logistic regression model after imputation with the 1000 Genomes reference panel. Although the r^2 shown here (and in 4B below) suggests more localized LD between variants, the D' suggests that these variants are inherited on low-frequency haplotypes. SNP order used to adjust for each step is as given in Table 3.

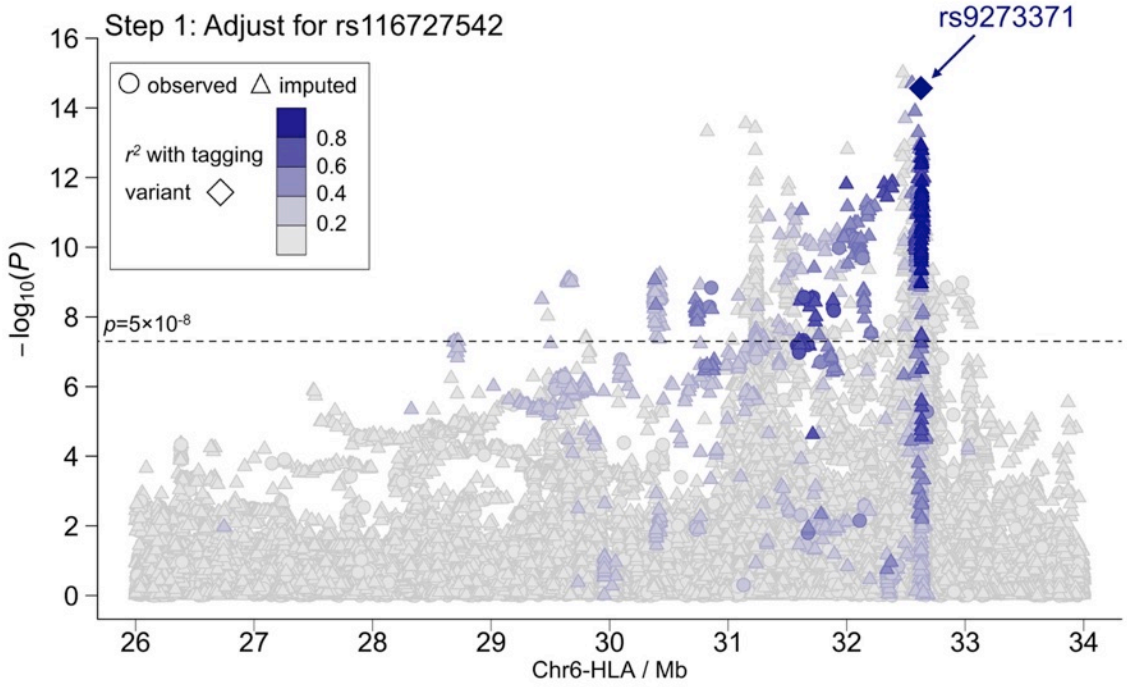

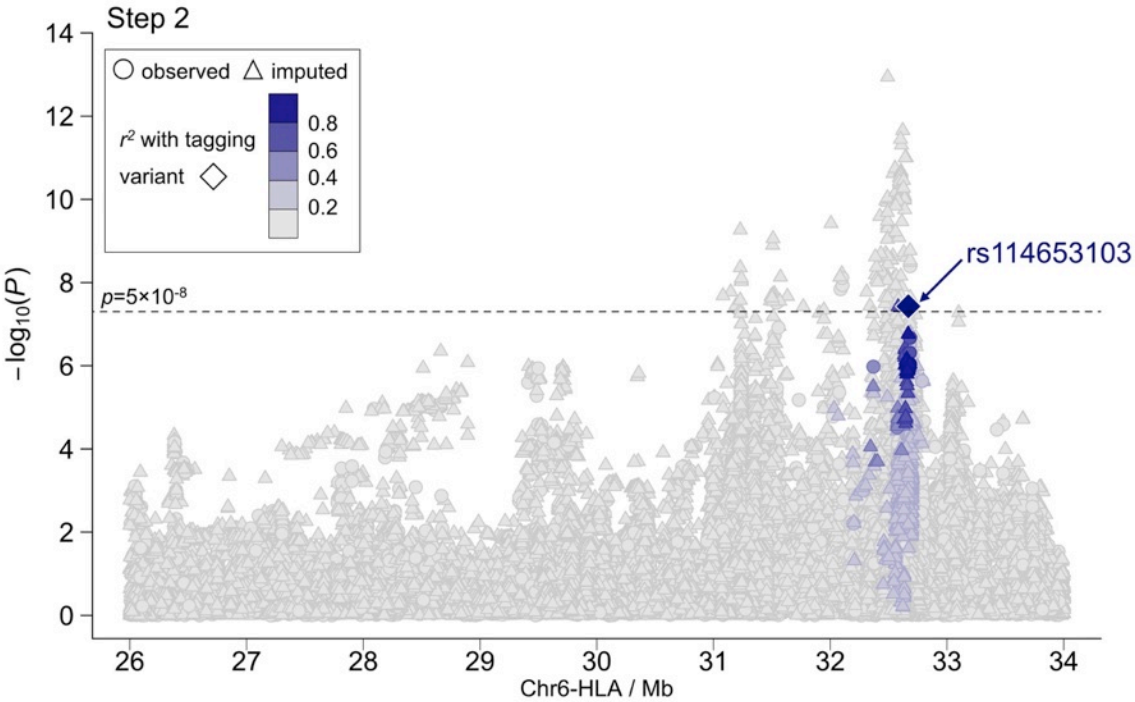

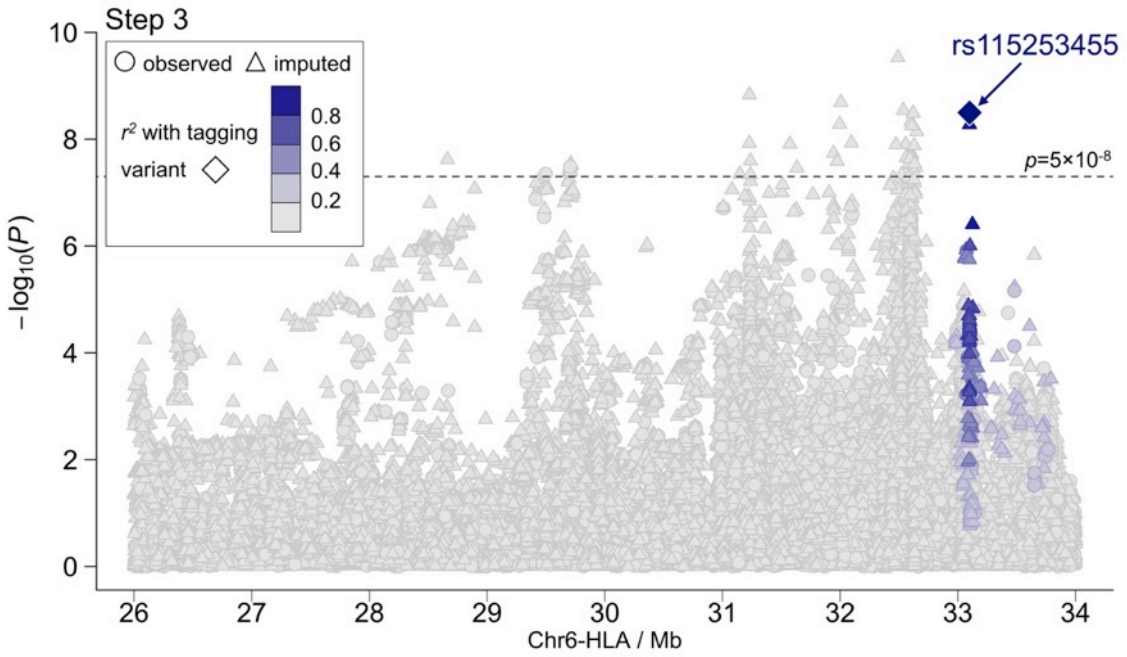
Step 3
observed
imputed
r^2 with tagging variant
0.8
0.6
0.4
0.2
rs115253455
$p=5\times10^{-8}$
$-\log_{10}(P)$
Chr6-HLA / Mb

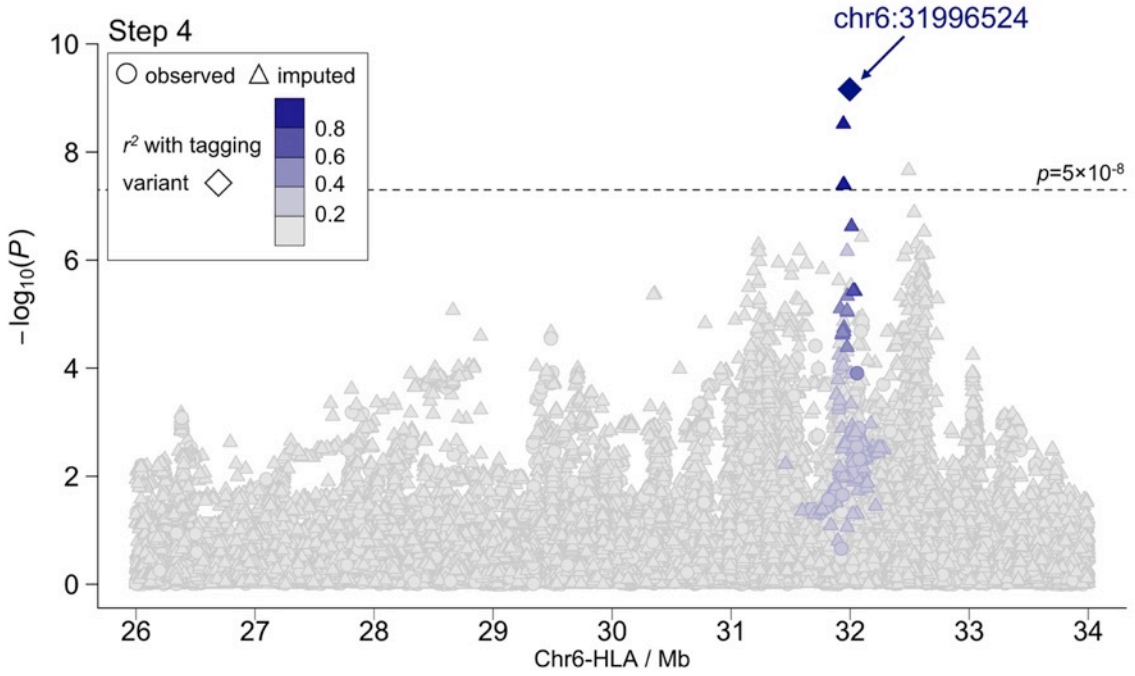
Step 4
observed
imputed
r^2 with tagging variant
0.8
0.6
0.4
0.2
chr6:31996524
$p=5\times10^{-8}$
$-\log_{10}(P)$
Chr6-HLA / Mb

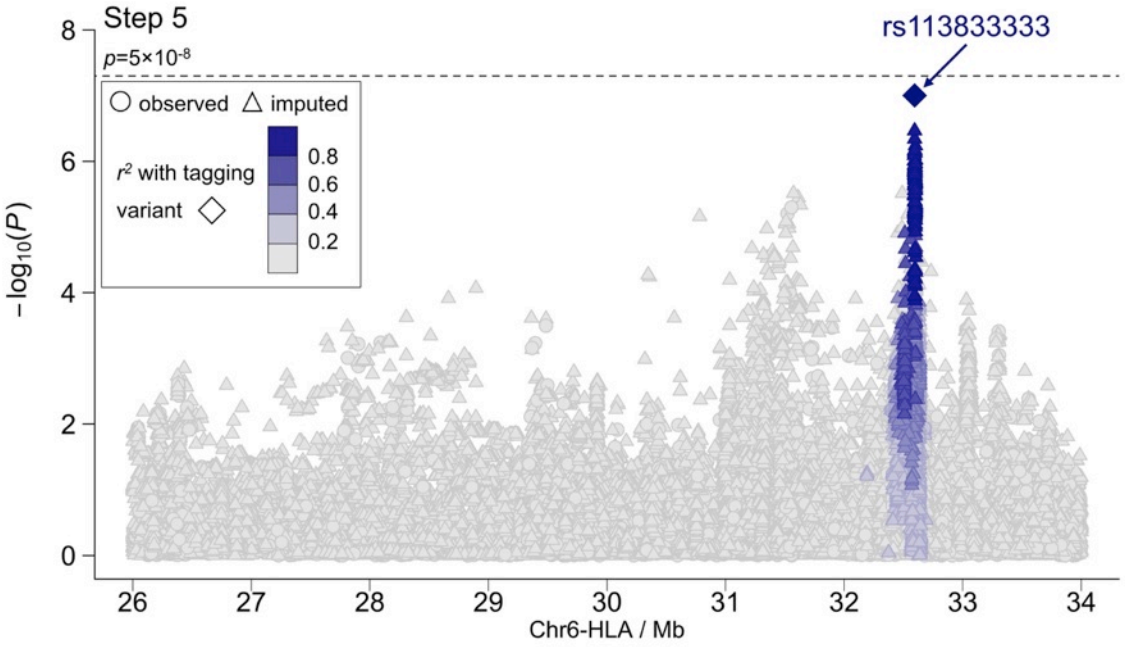
Step 5
p=5×10-8
rs113833333
observed
imputed
r2 with tagging variant
0.8
0.6
0.4
0.2
−log10(P)
Chr6-HLA / Mb

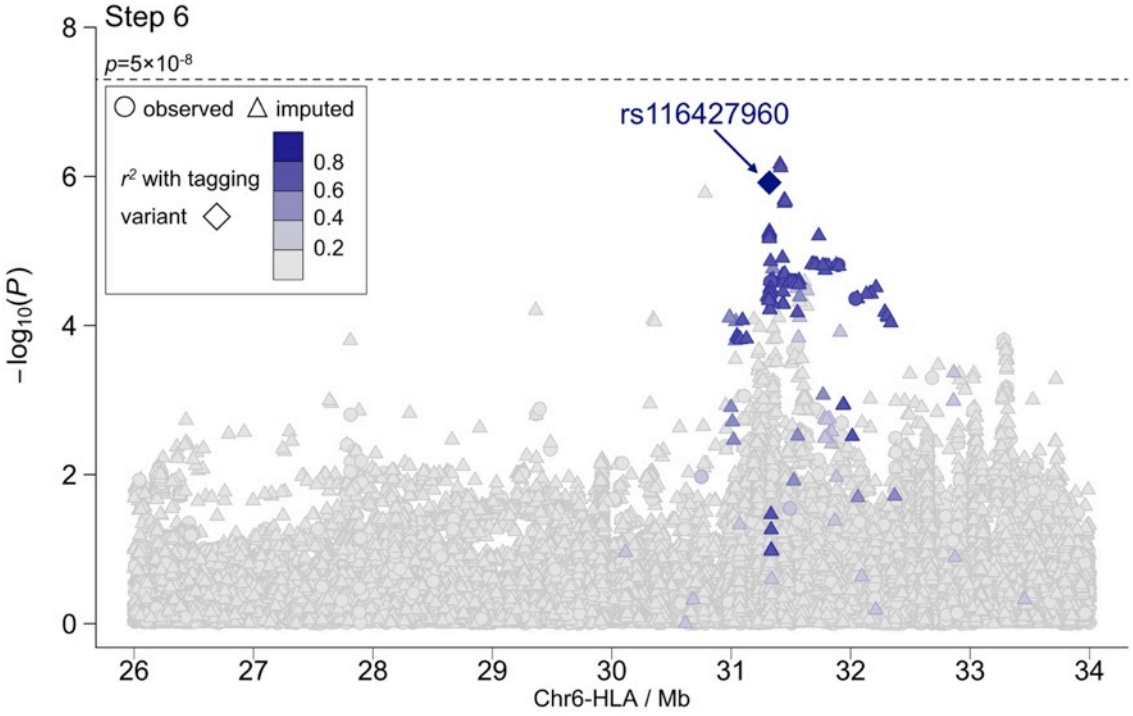
Step 6
p=5×10-8
rs116427960
observed
imputed
r2 with tagging variant
0.8
0.6
0.4
0.2
−log10(P)
Chr6-HLA / Mb

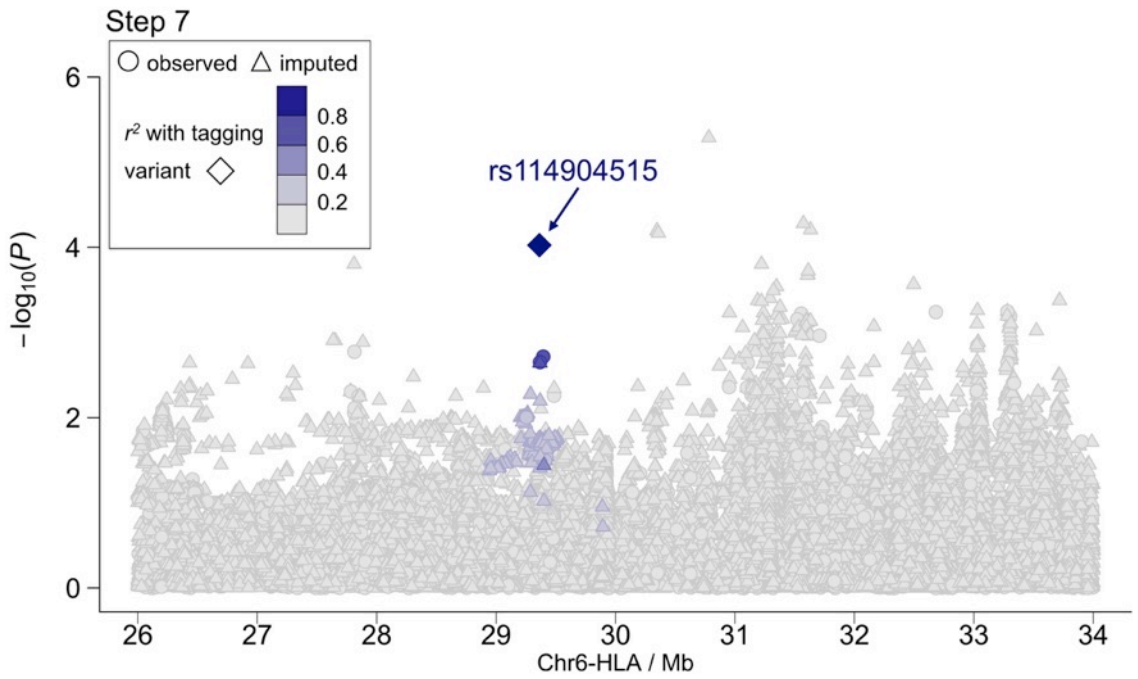
Step 7
observed
imputed
r2 with tagging variant
0.8
0.6
0.4
0.2
rs114904515
−log10(P)
0
2
4
6
26
27
28
29
30
31
32
33
34
Chr6-HLA / Mb

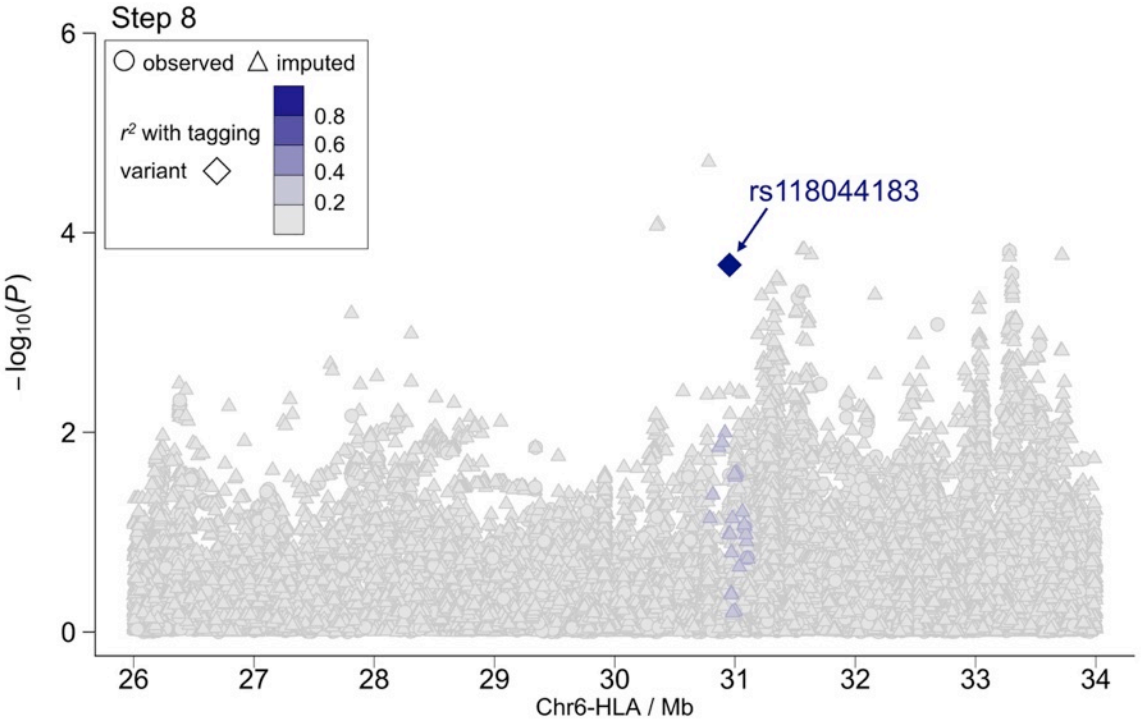
Step 8
observed
imputed
r2 with tagging variant
0.8
0.6
0.4
0.2
rs118044183
−log10(P)
0
2
4
6
26
27
28
29
30
31
32
33
34
Chr6-HLA / Mb

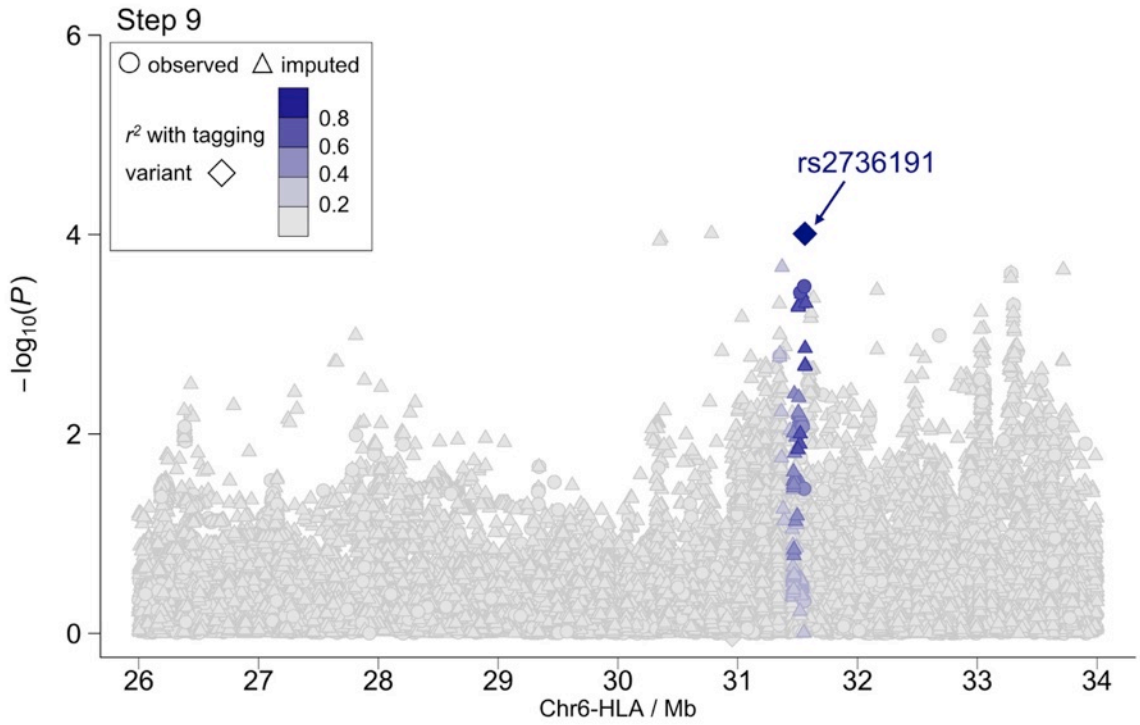
Step 9
observed
imputed
r2 with tagging variant
0.8
0.6
0.4
0.2
rs2736191
−log10(P)
Chr6-HLA / Mb

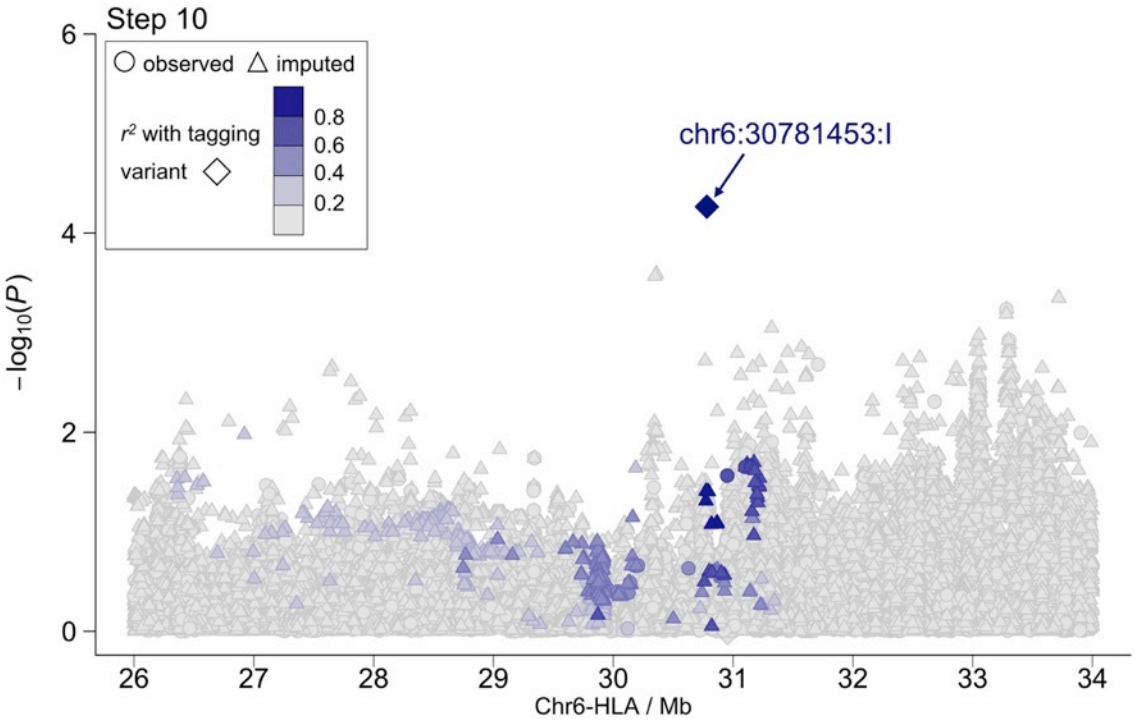
Step 10
observed
imputed
r2 with tagging variant
0.8
0.6
0.4
0.2
chr6:30781453:I
−log10(P)
Chr6-HLA / Mb

Supplementary Figure 4B: Results after stepwise analysis of the HLA region after imputation. Below are the $-\log_{10}$(P-value) for the results after each variant added to the stepwise logistic regression model after imputation using HiBAG for the classical HLA alleles. These plots illustrate the effect on the variants identified in the GWAS when adjusting for the HLA classical alleles. Allele order used to adjust for each step is as given in Table 4.

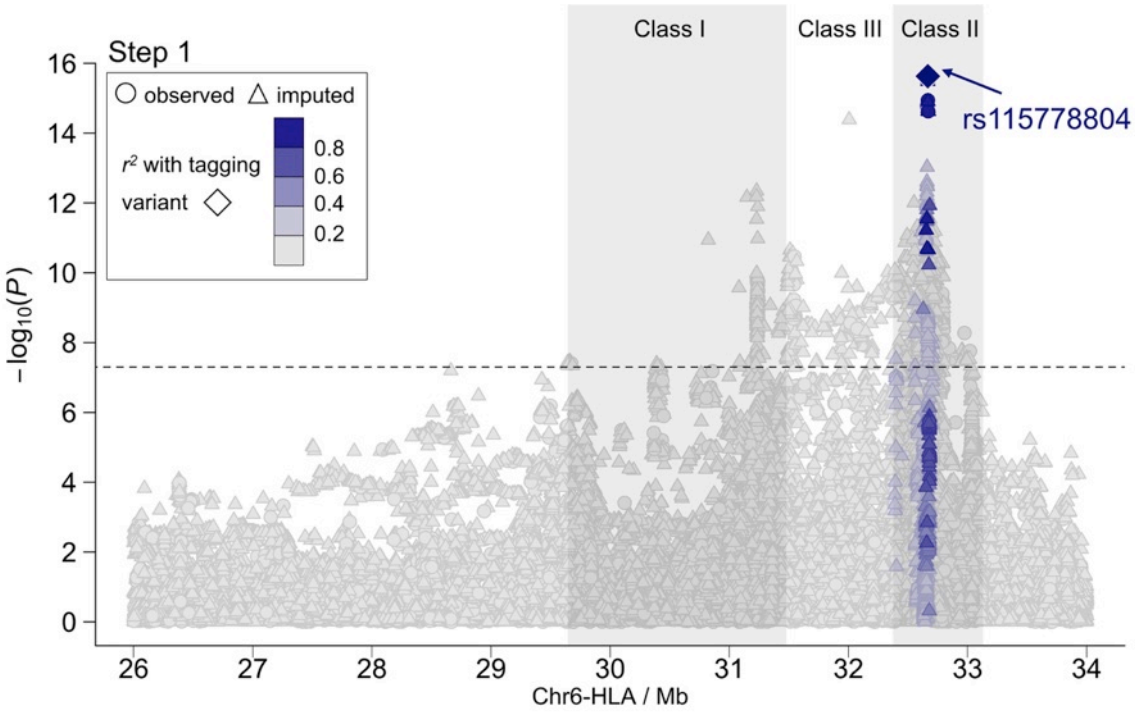

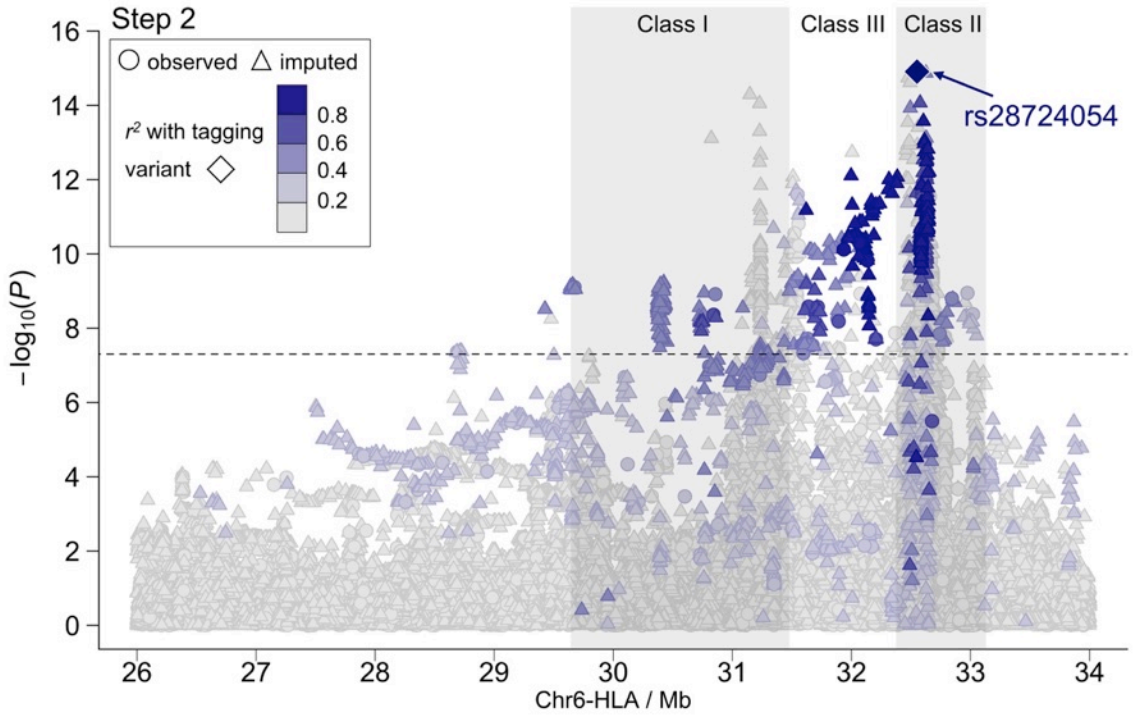

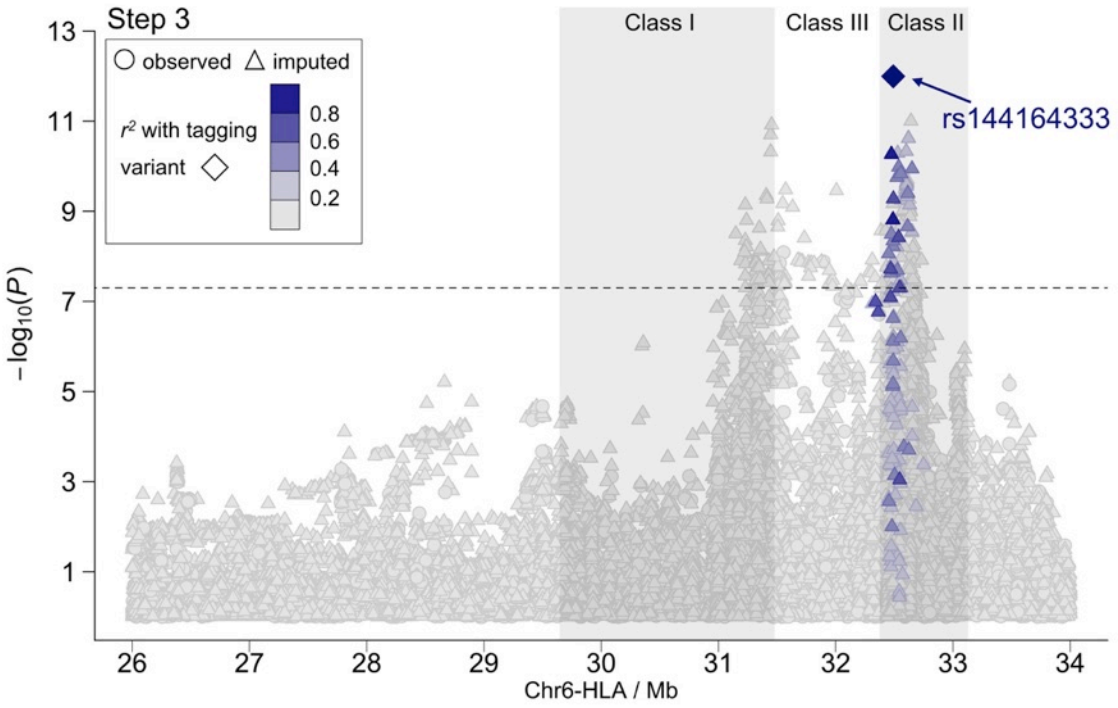
Step 3
Class I
Class III
Class II
observed
imputed
r^2 with tagging variant
0.8
0.6
0.4
0.2
rs144164333
$-\log_{10}(P)$
Chr6-HLA / Mb

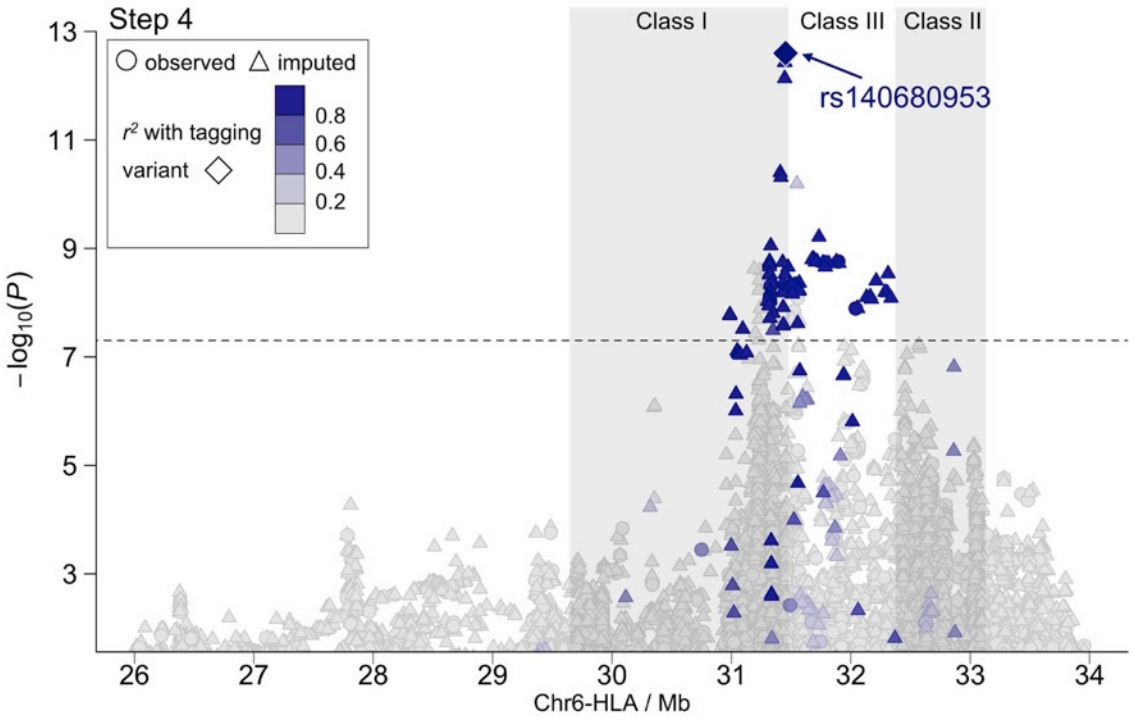
Step 4
Class I
Class III
Class II
observed
imputed
r^2 with tagging variant
0.8
0.6
0.4
0.2
rs140680953
$-\log_{10}(P)$
Chr6-HLA / Mb

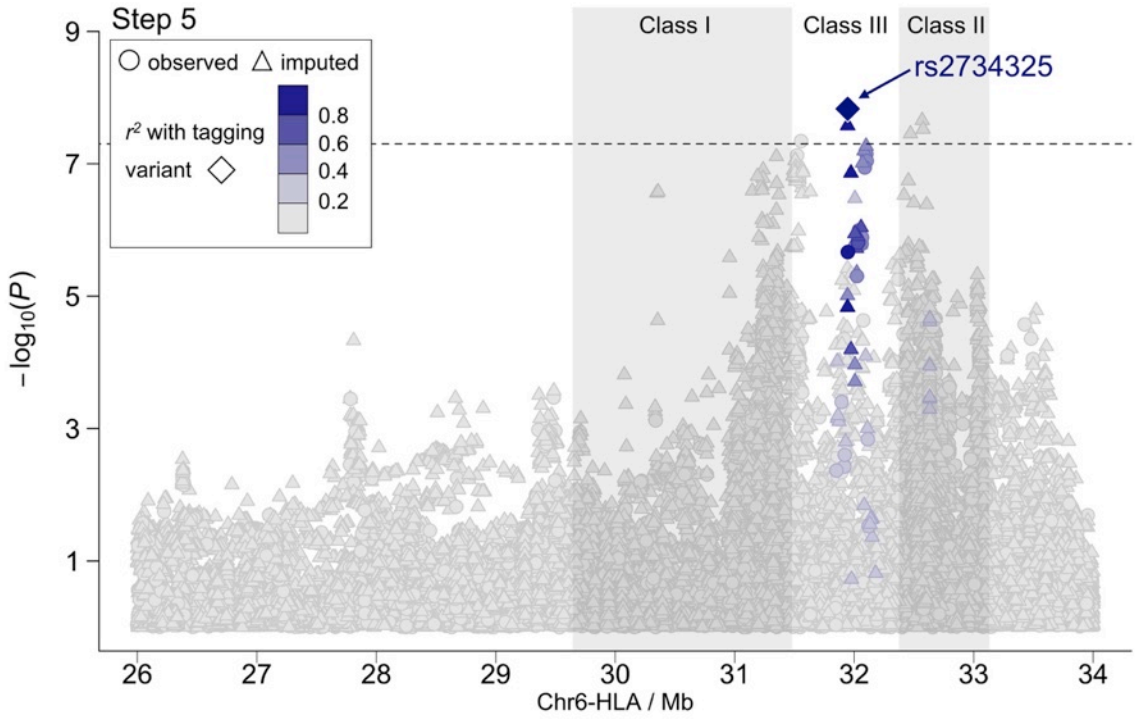
Step 5
Class I
Class III
Class II
rs2734325
observed
imputed
r^2 with tagging variant
0.8
0.6
0.4
0.2
$-\log_{10}(P)$
Chr6-HLA / Mb

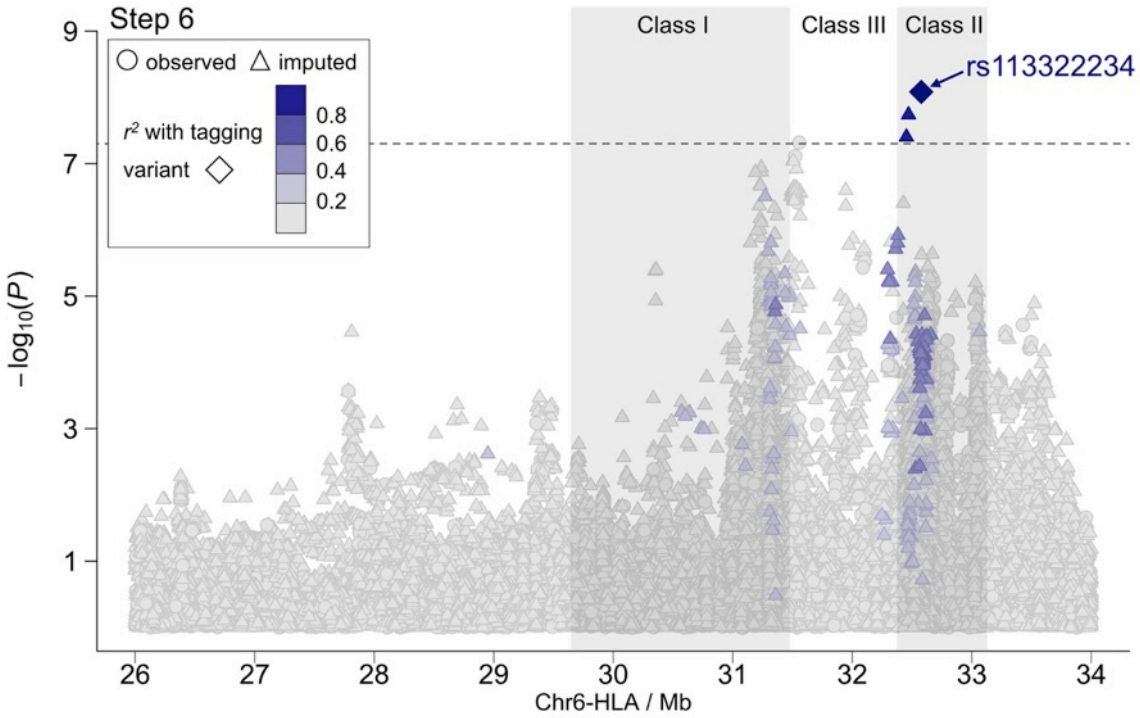
Step 6
Class I
Class III
Class II
rs113322234
observed
imputed
r^2 with tagging variant
0.8
0.6
0.4
0.2
$-\log_{10}(P)$
Chr6-HLA / Mb

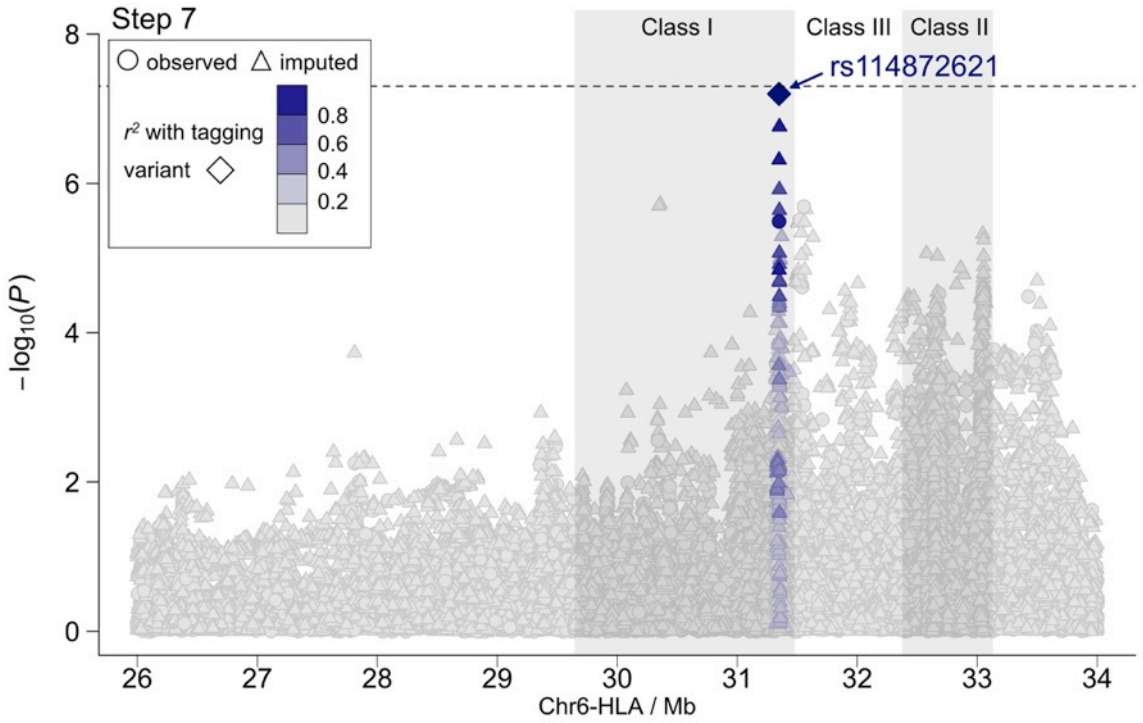
Step 7
Class I
Class III
Class II
rs114872621
observed
imputed
r2 with tagging variant
0.8
0.6
0.4
0.2
−log10(P)
Chr6-HLA / Mb

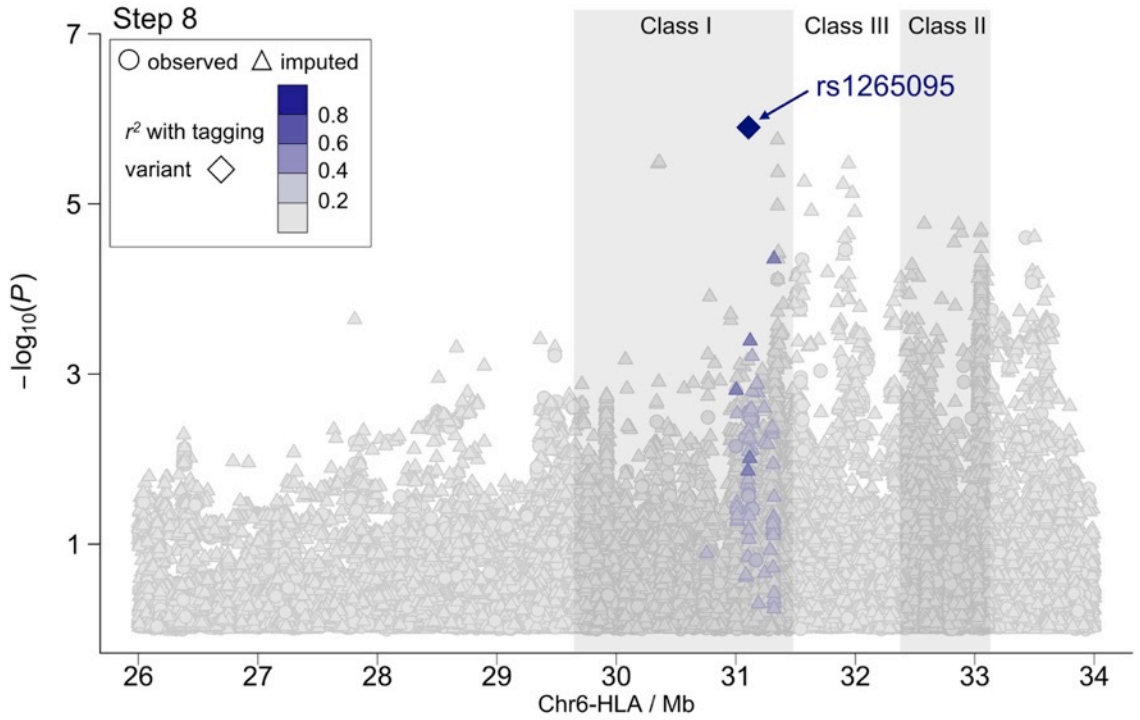
Step 8
Class I
Class III
Class II
rs1265095
observed
imputed
r2 with tagging variant
0.8
0.6
0.4
0.2
−log10(P)
Chr6-HLA / Mb

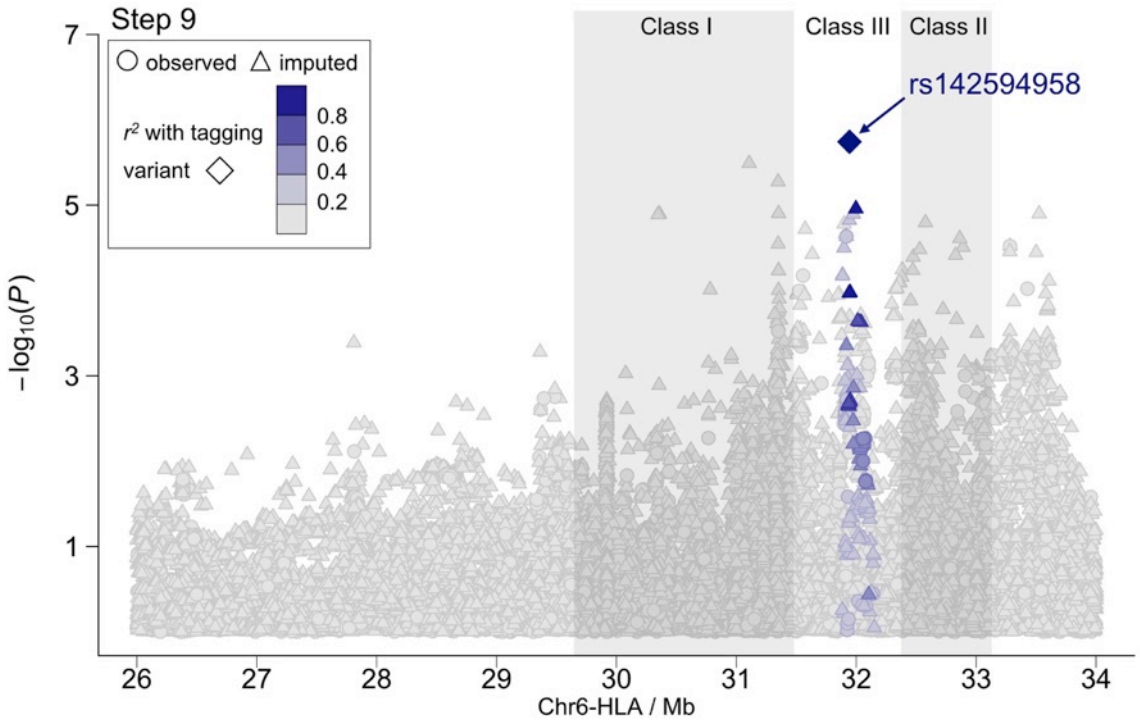
Step 9
observed
imputed
r^2 with tagging variant
0.8
0.6
0.4
0.2
Class I
Class III
Class II
rs142594958
$-\log_{10}(P)$
Chr6-HLA / Mb

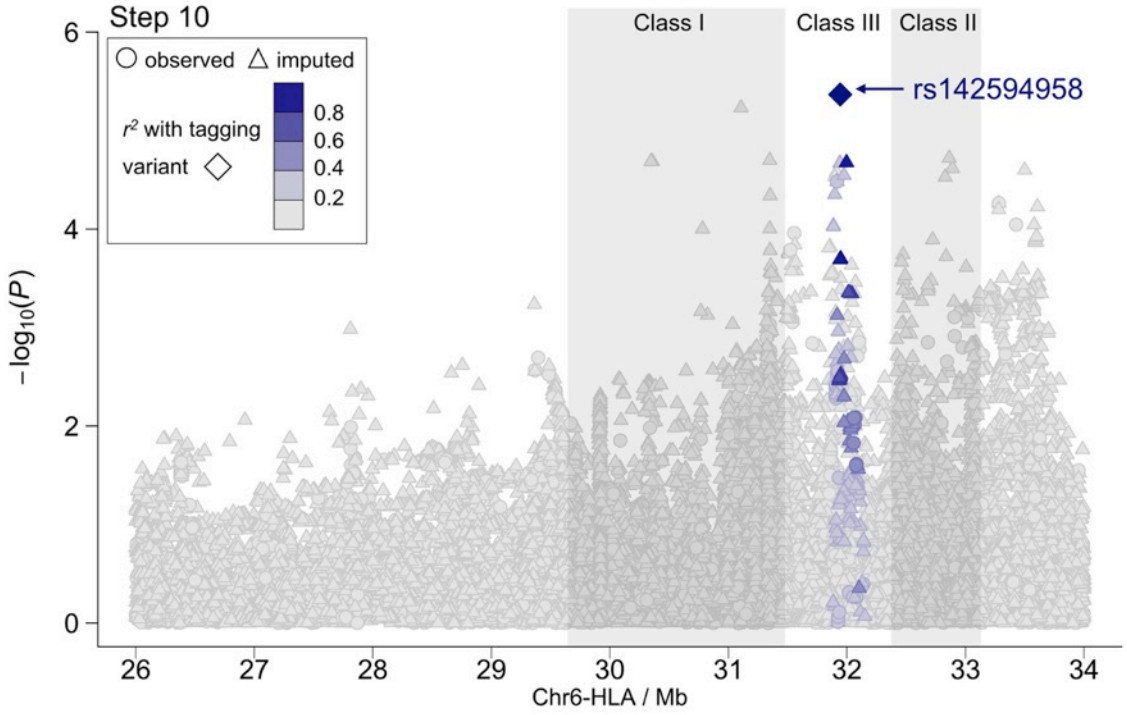
Step 10
observed
imputed
r^2 with tagging variant
0.8
0.6
0.4
0.2
Class I
Class III
Class II
rs142594958
$-\log_{10}(P)$
Chr6-HLA / Mb

Supplementary Table 5: Results of HLA classical allele imputation using HiBAG.

	Dosage Frequency		Best Guess count				
HLA Allele	Cases	Controls	Cases	Controls	Odds Ratio	95% CI	P-value
A*30:01	0.0749	0.0535	88	227	1.42	1.10 - 1.83	6.49E-03
A*03:02	0.0079	0.0028	10	13	3.48	1.35 - 8.95	9.83E-03
A*33:03	0.2857	0.3212	338	1365	0.87	0.77 - 0.99	3.75E-02
A*32:01	0.0092	0.0157	10	64	0.52	0.25 - 1.08	7.87E-02
A*02:03	0.0517	0.0467	27	65	1.42	0.84 - 2.38	1.92E-01
A*03:01	0.0386	0.0311	45	132	1.26	0.89 - 1.78	2.01E-01
A*31:01	0.1211	0.1081	141	459	1.13	0.93 - 1.38	2.19E-01
A*02:07	0.0809	0.0747	93	314	1.12	0.85 - 1.48	4.16E-01
A*24:02	0.3950	0.4092	518	1938	0.95	0.84 - 1.08	4.17E-01
A*11:01	0.2149	0.2042	260	887	1.06	0.91 - 1.24	4.49E-01
A*26:01	0.0942	0.1003	157	625	0.91	0.70 - 1.18	4.77E-01
A*02:06	0.1709	0.1635	214	739	1.06	0.89 - 1.27	5.33E-01
A*01:01	0.0316	0.0349	37	148	0.89	0.62 - 1.30	5.58E-01
A*02:01	0.2644	0.2720	357	1332	0.96	0.82 - 1.12	5.89E-01
A*30:04	0.0236	0.0248	28	107	0.95	0.62 - 1.45	7.98E-01
A*68:01	0.0041	0.0037	4	13	1.15	0.35 - 3.79	8.16E-01
A*29:01	0.0117	0.0112	14	49	1.06	0.55 - 2.07	8.56E-01
B*08:01	0.0165	0.0036	20	14	5.43	2.66 - 11.08	3.42E-06
B*15:01	0.1149	0.1550	205	985	0.55	0.42 - 0.71	7.51E-06
B*40:06	0.1039	0.0788	111	283	1.55	1.20 - 2.02	9.53E-04
B*39:01	0.0289	0.0172	37	70	2.36	1.40 - 3.98	1.27E-03
B*67:01	0.0252	0.0152	41	88	2.39	1.35 - 4.24	2.82E-03
B*13:01	0.0263	0.0437	31	179	0.52	0.34 - 0.81	3.38E-03
B*55:02	0.0276	0.0371	48	248	0.36	0.17 - 0.73	4.79E-03
B*38:02	0.0447	0.0317	47	119	1.66	1.13 - 2.43	9.90E-03
B*52:01	0.0454	0.0640	48	255	0.67	0.48 - 0.92	1.35E-02
B*51:01	0.2124	0.1817	262	826	1.23	1.04 - 1.44	1.41E-02
B*13:02	0.0772	0.0588	90	248	1.34	1.04 - 1.72	2.15E-02
B*58:01	0.0978	0.1221	116	526	0.78	0.63 - 0.96	2.15E-02
B*40:02	0.0923	0.0788	142	439	1.34	1.00 - 1.81	4.92E-02
B*35:01	0.1219	0.1046	168	518	1.22	0.98 - 1.52	6.98E-02
B*40:01	0.0948	0.0794	113	340	1.23	0.97 - 1.55	8.36E-02
B*56:01	0.0067	0.0084	2	12	0.10	0.01 - 1.48	9.47E-02
B*51:02	0.0190	0.0154	18	38	1.76	0.80 - 3.87	1.62E-01
B*44:02	0.0278	0.0351	33	153	0.77	0.52 - 1.15	2.03E-01
B*15:02	0.0073	0.0100	5	27	0.45	0.13 - 1.58	2.12E-01
B*48:01	0.0472	0.0537	68	294	0.82	0.57 - 1.18	2.89E-01
B*54:01	0.1003	0.1098	134	522	0.88	0.70 - 1.12	3.05E-01
B*81:01	0.0031	0.0049	4	24	0.47	0.11 - 2.05	3.15E-01
B*37:01	0.0270	0.0325	31	139	0.82	0.55 - 1.22	3.17E-01
B*27:05	0.0452	0.0521	53	221	0.85	0.62 - 1.17	3.24E-01
B*07:02	0.0607	0.0683	75	309	0.88	0.67 - 1.15	3.53E-01

B*46:01	0.1060	0.0983	127	443	1.11	0.88 - 1.42	3.77E-01
B*27:04	0.0075	0.0065	5	14	1.63	0.42 - 6.39	4.84E-01
B*57:01	0.0056	0.0042	6	17	1.38	0.52 - 3.62	5.19E-01
B*15:11	0.0275	0.0288	15	43	0.80	0.34 - 1.88	6.06E-01
B*35:03	0.0253	0.0268	7	47	0.85	0.43 - 1.67	6.38E-01
B*44:03	0.1630	0.1684	196	730	0.97	0.82 - 1.14	6.91E-01
B*15:18	0.0289	0.0302	32	124	0.93	0.56 - 1.52	7.61E-01
B*14:01	0.0212	0.0225	26	101	0.93	0.57 - 1.51	7.65E-01
B*07:05	0.0162	0.0157	16	54	1.05	0.58 - 1.88	8.77E-01
C*07:01	0.0992	0.0645	120	276	1.64	1.30 - 2.07	3.03E-05
C*14:03	0.0650	0.1062	76	457	0.59	0.46 - 0.76	3.61E-05
C*07:02	0.2229	0.1695	261	711	1.37	1.17 - 1.59	5.45E-05
C*14:02	0.1841	0.1475	226	653	1.31	1.11 - 1.56	1.94E-03
C*04:01	0.0892	0.1200	111	528	0.71	0.57 - 0.89	3.13E-03
C*03:02	0.1021	0.1313	120	565	0.76	0.62 - 0.94	9.23E-03
C*12:02	0.0518	0.0678	52	262	0.72	0.53 - 0.98	3.75E-02
C*15:02	0.0698	0.0561	73	201	1.34	1.00 - 1.79	4.82E-02
C*01:02	0.2923	0.3226	359	1429	0.88	0.77 - 1.01	6.51E-02
C*06:02	0.1128	0.0981	133	417	1.17	0.95 - 1.43	1.44E-01
C*05:01	0.0274	0.0348	33	149	0.76	0.51 - 1.15	1.93E-01
C*03:04	0.1952	0.2091	232	901	0.91	0.77 - 1.08	2.72E-01
C*08:01	0.1550	0.1438	193	663	1.10	0.91 - 1.32	3.16E-01
C*12:03	0.0124	0.0144	13	57	0.82	0.43 - 1.58	5.53E-01
C*08:02	0.0227	0.0253	26	101	0.87	0.54 - 1.40	5.73E-01
C*03:03	0.2217	0.2152	268	932	1.04	0.89 - 1.23	6.26E-01
C*02:02	0.0138	0.0127	15	51	1.10	0.59 - 2.05	7.54E-01
C*15:05	0.0091	0.0086	15	51	1.11	0.48 - 2.60	8.09E-01
C*07:04	0.0187	0.0192	21	82	0.97	0.57 - 1.64	9.05E-01
DPB1*04:01	0.1028	0.1545	114	637	0.62	0.51 - 0.77	8.90E-06
DPB1*13:01	0.1300	0.0939	157	414	1.55	1.25 - 1.92	7.79E-05
DPB1*05:01	0.7922	0.7272	930	3092	1.16	1.05 - 1.28	2.87E-03
DPB1*09:01	0.0398	0.0603	51	281	0.62	0.44 - 0.86	4.86E-03
DPB1*02:01	0.4943	0.5476	630	2454	0.85	0.76 - 0.95	5.35E-03
DPB1*09:02	0.0169	0.0124	24	63	2.24	0.99 - 5.10	5.36E-02
DPB1*02:02	0.0854	0.0751	60	220	1.39	0.97 - 1.99	7.13E-02
DPB1*14:01	0.0441	0.0360	52	145	1.41	0.94 - 2.11	9.97E-02
DPB1*03:01	0.0380	0.0340	88	283	1.31	0.78 - 2.20	3.13E-01
DPB1*17:01	0.0331	0.0366	41	160	0.90	0.62 - 1.30	5.66E-01
DPB1*19:01	0.0062	0.0053	11	35	1.33	0.44 - 3.99	6.16E-01
DPB1*04:02	0.1393	0.1422	180	668	0.98	0.80 - 1.18	7.95E-01
DPB1*104:01	0.0178	0.0174	10	34	1.08	0.45 - 2.59	8.69E-01
DQA1*03:01	0.2331	0.3179	145	907	0.54	0.45 - 0.65	1.05E-10
DQA1*02:01	0.1908	0.1319	224	559	1.51	1.28 - 1.79	8.87E-07
DQA1*05:05	0.0902	0.1208	154	747	0.60	0.46 - 0.79	3.20E-04
DQA1*03:02	0.1868	0.1558	286	847	1.41	1.15 - 1.75	1.27E-03
DQA1*01:02	0.4097	0.3572	475	1500	1.20	1.07 - 1.36	2.45E-03
DQA1*06:01	0.0549	0.0783	62	329	0.66	0.49 - 0.88	4.84E-03

DQA1*04:01	0.0432	0.0296	54	133	1.73	1.17 - 2.57	5.94E-03
DQA1*01:03	0.2599	0.2232	306	946	1.20	1.04 - 1.39	1.11E-02
DQA1*05:03	0.0176	0.0240	23	104	0.50	0.24 - 1.03	5.94E-02
DQA1*03:03	0.1354	0.1514	219	895	0.82	0.65 - 1.03	9.16E-02
DQA1*01:05	0.0220	0.0292	27	141	0.70	0.43 - 1.13	1.46E-01
DQA1*01:01	0.1681	0.1836	164	629	0.89	0.75 - 1.07	2.07E-01
DQA1*01:04	0.0806	0.0892	129	523	0.86	0.65 - 1.13	2.75E-01
DQA1*05:08	0.0245	0.0228	23	68	1.16	0.64 - 2.08	6.28E-01
DQA1*05:01	0.0777	0.0758	57	161	1.04	0.76 - 1.42	7.98E-01
DQB1*06:02	0.2492	0.1468	301	636	1.90	1.62 - 2.21	5.55E-16
DQB1*03:02	0.1244	0.2165	144	923	0.53	0.44 - 0.64	2.00E-11
DQB1*02:02	0.1798	0.1180	212	502	1.60	1.35 - 1.90	7.57E-08
DQB1*06:04	0.0612	0.0996	72	422	0.58	0.45 - 0.76	5.98E-05
DQB1*03:01	0.2485	0.3095	296	1327	0.75	0.65 - 0.87	1.10E-04
DQB1*03:03	0.2600	0.2168	306	917	1.26	1.09 - 1.46	1.95E-03
DQB1*06:09	0.0534	0.0769	62	345	0.65	0.48 - 0.87	3.96E-03
DQB1*06:01	0.2299	0.1914	268	807	1.22	1.06 - 1.41	6.51E-03
DQB1*04:01	0.1286	0.1593	150	667	0.77	0.64 - 0.94	9.11E-03
DQB1*04:02	0.0728	0.0593	88	263	1.34	1.00 - 1.79	5.12E-02
DQB1*05:01	0.1607	0.1804	189	767	0.88	0.75 - 1.04	1.39E-01
DQB1*02:01	0.0451	0.0370	53	156	1.23	0.89 - 1.70	2.04E-01
DQB1*05:02	0.0728	0.0637	82	259	1.17	0.90 - 1.52	2.42E-01
DQB1*05:03	0.0758	0.0841	86	357	0.89	0.70 - 1.14	3.60E-01
DQB1*06:03	0.0340	0.0366	39	144	0.91	0.62 - 1.35	6.38E-01
DRB1*15:01	0.2642	0.1572	312	667	1.85	1.59 - 2.14	5.55E-16
DRB1*04:06	0.0331	0.0669	41	354	0.15	0.09 - 0.26	2.63E-11
DRB1*04:03	0.0414	0.0752	55	360	0.18	0.11 - 0.30	8.83E-11
DRB1*08:03	0.1955	0.1321	251	613	1.59	1.34 - 1.88	7.37E-08
DRB1*13:02	0.1142	0.1794	134	765	0.61	0.51 - 0.74	4.60E-07
DRB1*07:01	0.1911	0.1320	225	559	1.52	1.29 - 1.80	7.28E-07
DRB1*11:01	0.0532	0.0820	75	453	0.52	0.37 - 0.72	1.12E-04
DRB1*12:02	0.0391	0.0658	39	266	0.52	0.37 - 0.74	2.98E-04
DRB1*09:01	0.2357	0.1928	287	851	1.27	1.10 - 1.48	1.64E-03
DRB1*16:02	0.0343	0.0222	38	87	1.78	1.16 - 2.72	7.73E-03
DRB1*04:05	0.1313	0.1621	156	696	0.78	0.64 - 0.94	9.48E-03
DRB1*04:04	0.0263	0.0354	22	89	0.44	0.22 - 0.86	1.67E-02
DRB1*08:02	0.0540	0.0396	70	182	1.48	1.07 - 2.04	1.85E-02
DRB1*01:01	0.1064	0.1276	125	546	0.82	0.68 - 1.01	5.91E-02
DRB1*14:04	0.0189	0.0239	20	109	0.50	0.23 - 1.10	8.66E-02
DRB1*10:01	0.0264	0.0361	30	147	0.70	0.47 - 1.06	9.34E-02
DRB1*15:02	0.0650	0.0793	73	326	0.81	0.62 - 1.05	1.06E-01
DRB1*03:01	0.0448	0.0373	53	156	1.21	0.88 - 1.67	2.40E-01
DRB1*14:03	0.0175	0.0213	21	85	0.73	0.40 - 1.35	3.14E-01
DRB1*04:01	0.0222	0.0192	26	61	1.32	0.71 - 2.43	3.80E-01
DRB1*14:01	0.0315	0.0348	47	182	0.78	0.44 - 1.38	3.85E-01
DRB1*12:01	0.1008	0.1068	116	459	0.92	0.73 - 1.17	5.08E-01
DRB1*13:01	0.0337	0.0363	37	145	0.92	0.63 - 1.33	6.53E-01

DRB1*14:05	0.0428	0.0442	65	233	0.95	0.64 - 1.42	8.03E-01
DRB1*04:10	0.0188	0.0190	25	80	0.97	0.45 - 2.11	9.43E-01

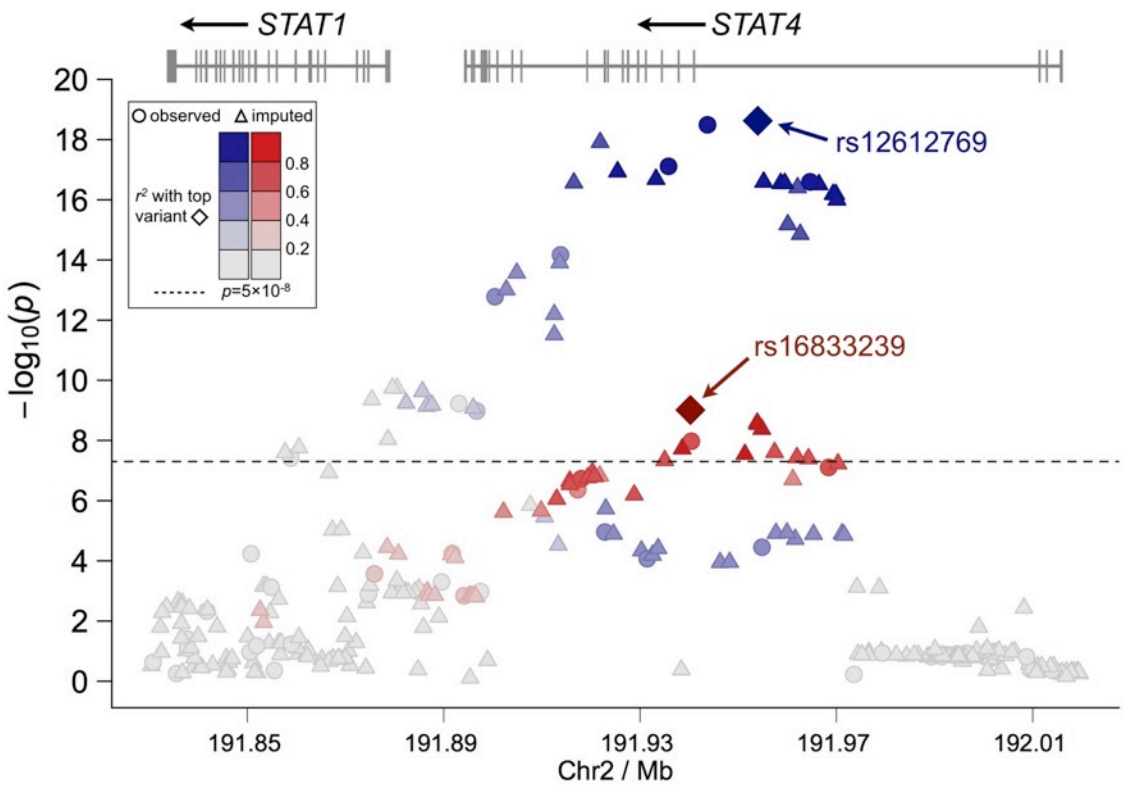

Supplementary Figure 5: Zoom plot of the single locus analysis with SLE after imputation in the region of *STAT4*. In the region of *STAT1* and *STAT4* after imputation, two independent signals were observed in the stepwise regression model, with rs12612769 being the most significant, which is located in the third intron of *STAT4* (blue diamond; r^2 with this variant is given in blue). The variant rs12612769 was in strong LD with a previously reported association of Han Chinese SLE cases[9], rs7574865, with r^2 = 0.97 and *D'*=0.93. The second effect identified by the stepwise regression analysis was tagged by rs16833239 (red diamond; r^2 with this variant is given in red).

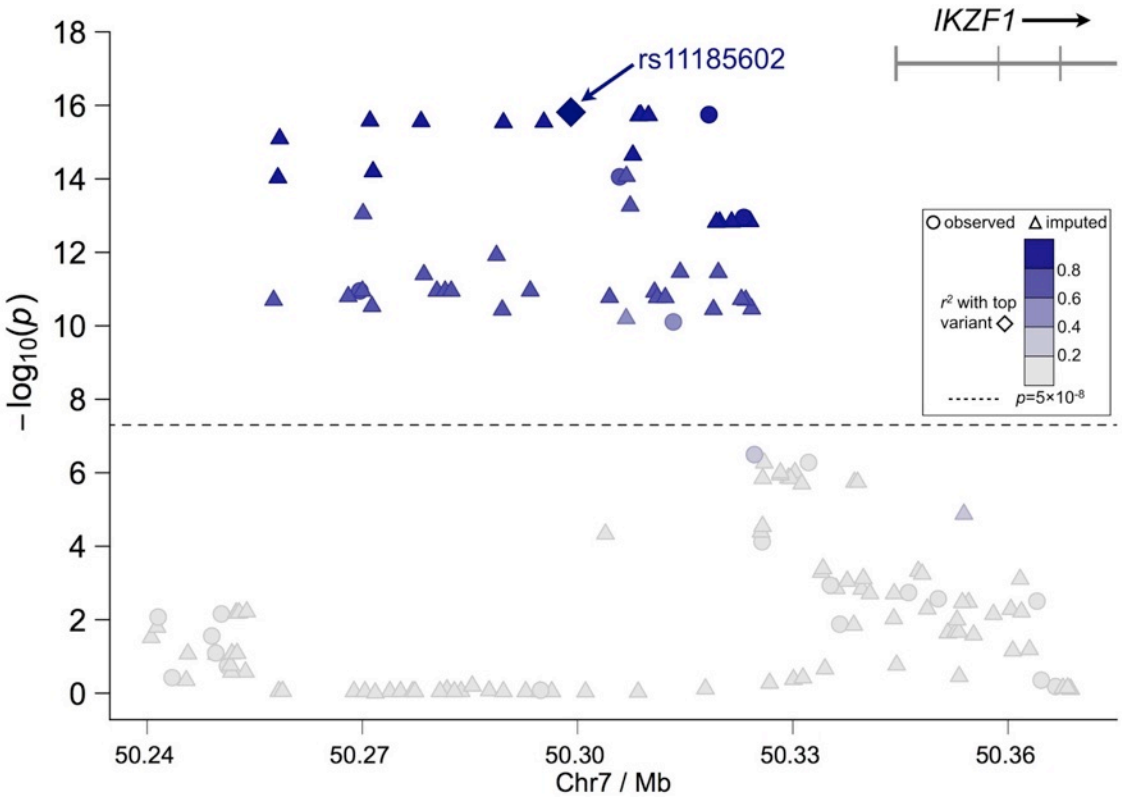

Supplementary Figure 6: Zoom plot of the single locus analysis with SLE after imputation in the region of *IKZF1.* In the region of *IKZF1* after imputation, only one independent signal was observed in the stepwise model peaking at rs11185602 (blue diamond; r^2 with this variant is given in blue) located in the proximal promoter region of the locus. These data are consistent with the previously published studies in Han Chinese[9] reporting rs4917014 with D' = 1.0 and r^2 = 0.75 with rs11185602, identified here in Koreans.

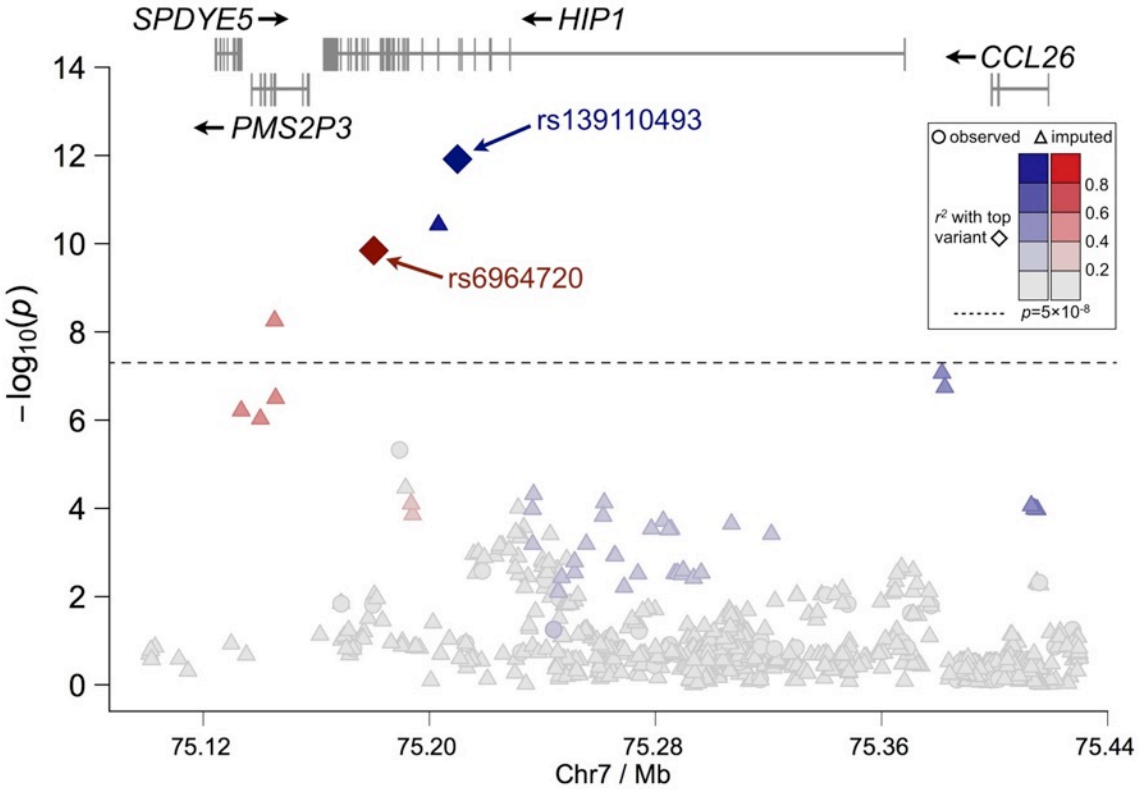

Supplementary Figure 7: Zoom plot of the single locus analysis with SLE after imputation in the region of *HIP1.* In the region of *HIP1* after imputation, two independent effects were identified in the stepwise model. The first effect was accounted for by rs139110493 (blue diamond; r^2 with this variant is given in blue) located within the 7th intron of the *HIP1* coding region, and rs6964720 (red diamond; r^2 with this variant is given in red) within the 22nd intron accounted for the second effect. In the GWAS in Han Chinese SLE subjects[9], rs1167796 was identified in this region. Although the r^2 between rs1167796 variants was only <0.15, the variants are in strong D' greater than 0.85 indicating they are inherited on a common haplotype.

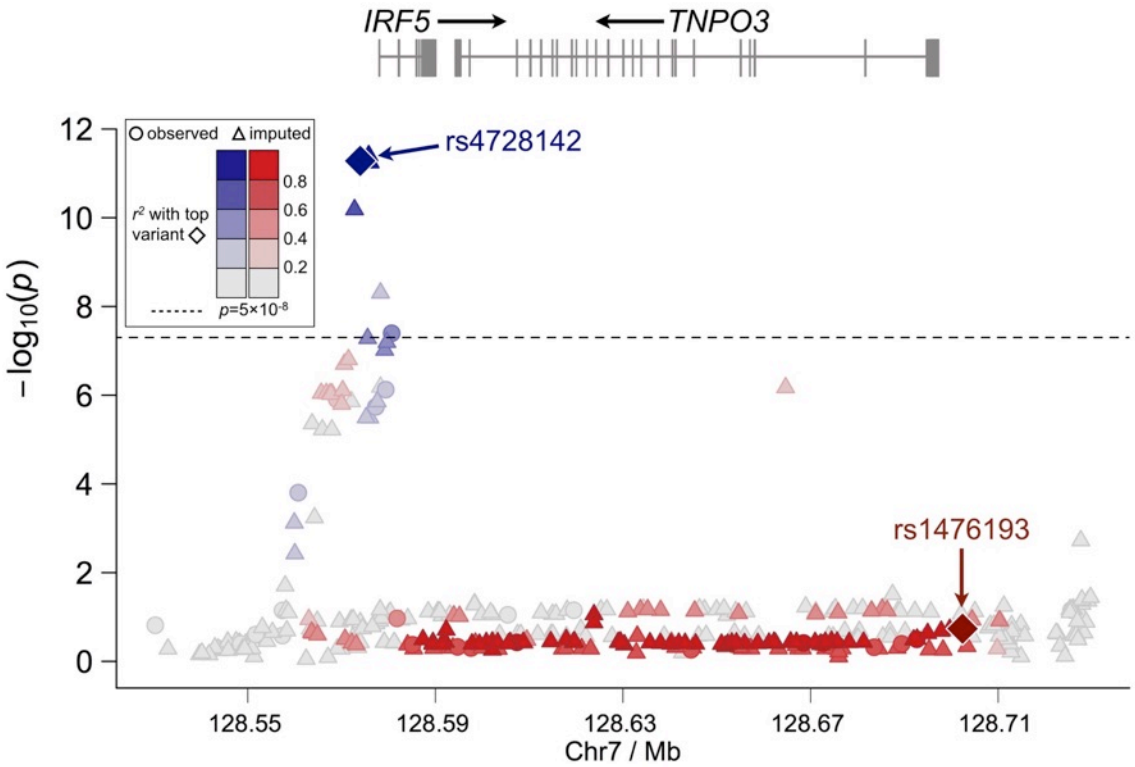

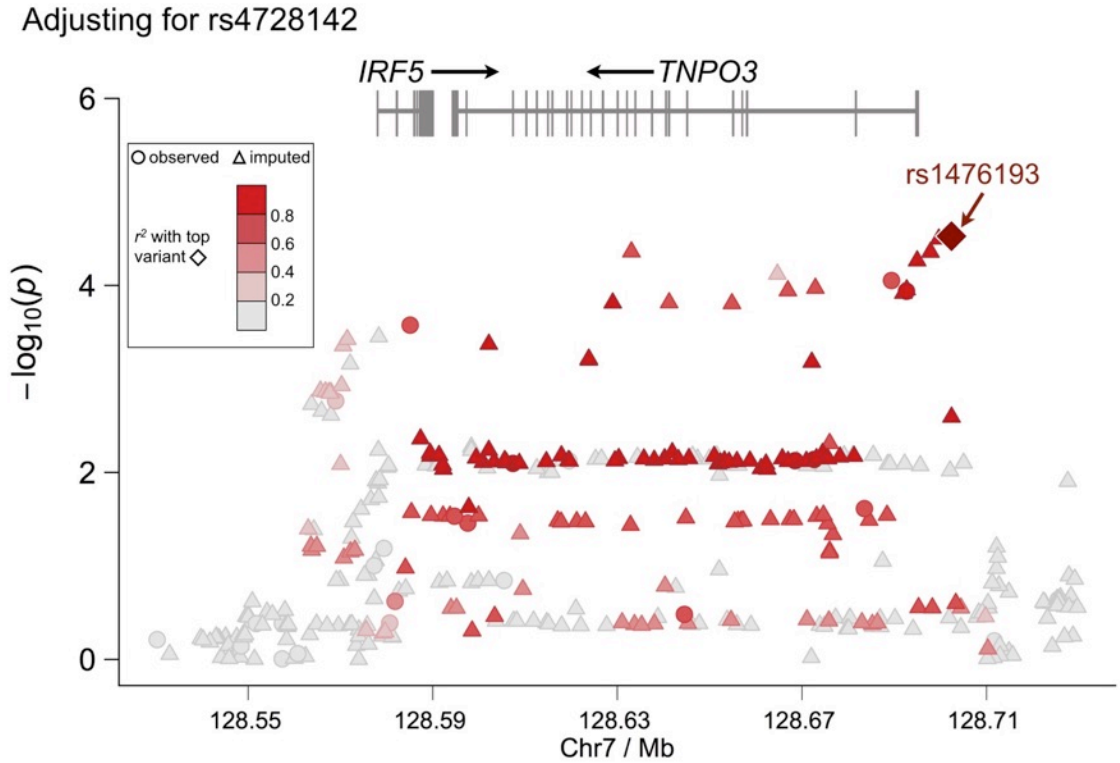

Supplementary Figure 8: Zoom plot of the single locus analysis with SLE after imputation in the region of *IRF5.* In the region of IRF5 after imputation, two independent effects were identified in the stepwise model. The first independent effect was accounted for by rs4728142 (blue diamond; r^2 with this variant is given in blue) located in the promoter region of IRF5. After adjusting for rs4728142, a set of variants became significant that showed no association in the univariate analysis, peaking at rs1476193 (red diamond; r^2 with this variant is given in red) located in the promoter region of TNPO3.

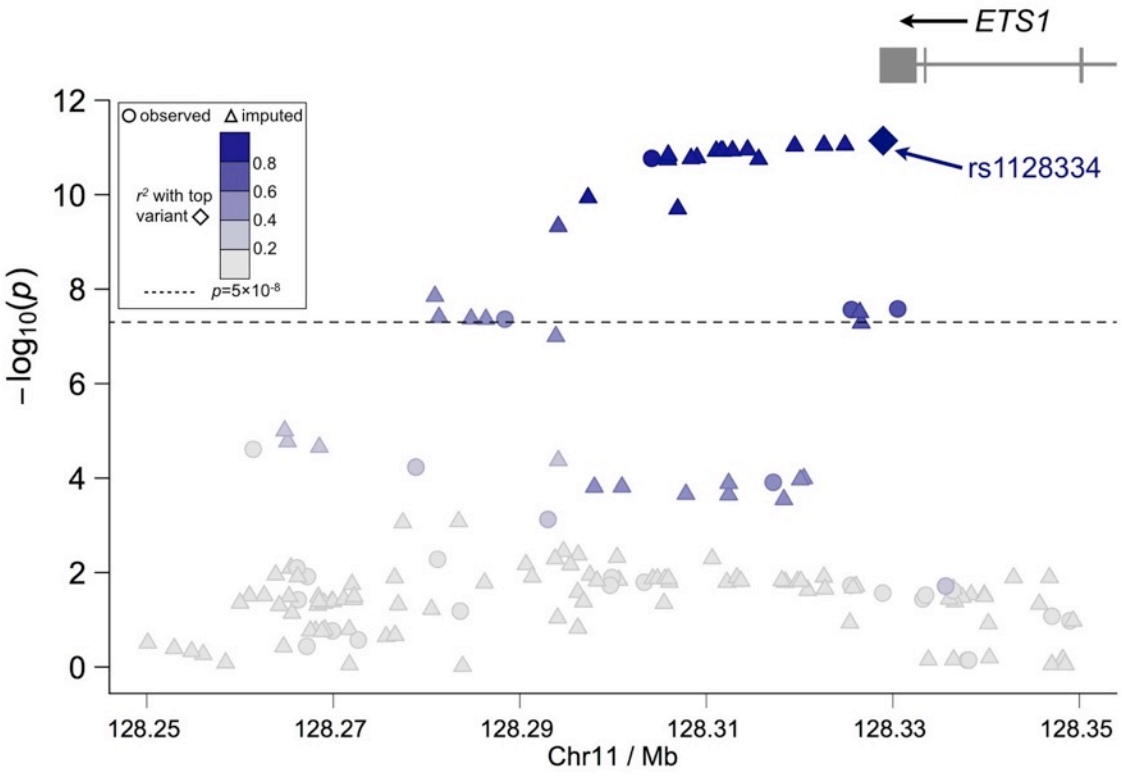

Supplementary Figure 9: Zoom plot of the single locus analysis with SLE after imputation in the region of *ETS1.* In the region of *ETS1* after imputation, only a single independent effect was identified in the stepwise model lead by rs1128334 (blue diamond). In the previous GWAS in Han Chinese[9], rs6590330 was the variant reported. The linkage disequilibrium between rs1128334 and rs6590330 is r^2=0.98 and D'=0.99, indicating that these variants represent a single effect.

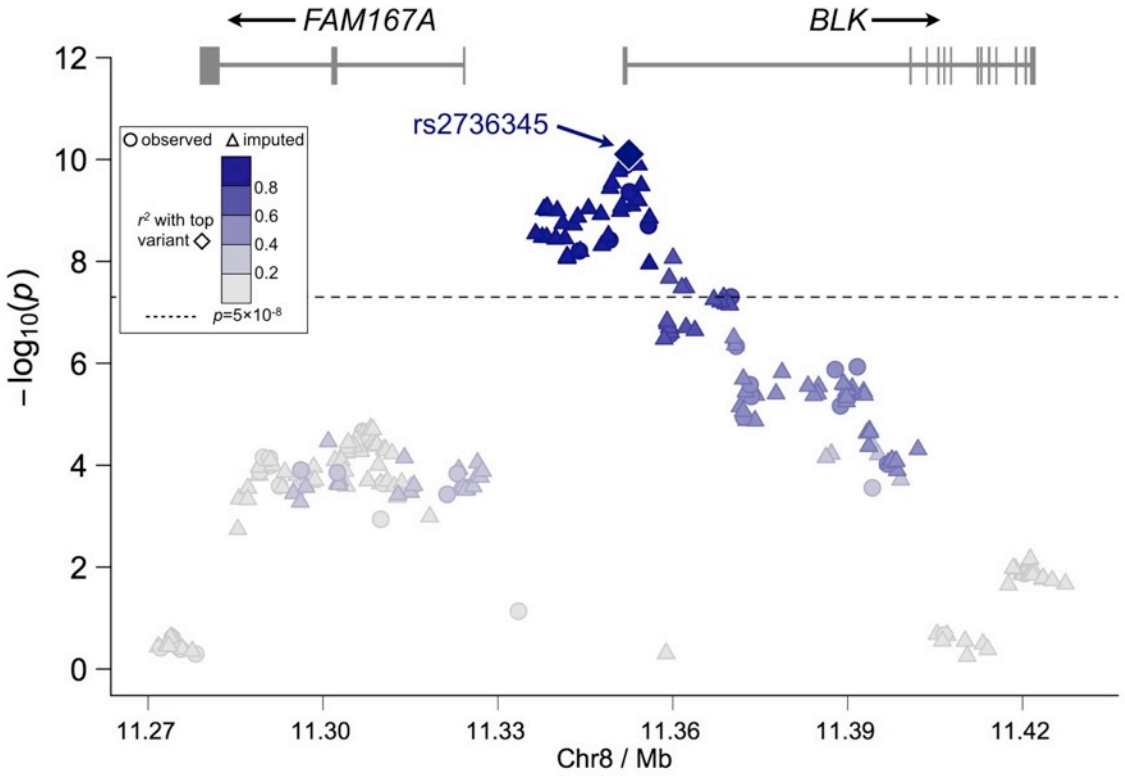

Supplementary Figure 10: Zoom plot of the single locus analysis with SLE after imputation in the region of *BLK.* In the region of *BLK* after imputation, only a single independent effect was identified in the stepwise model lead by rs2736345 (blue diamond). Several studies have been published looking at this region in Asians. The Han Chinese GWAS[9] reported rs7812879, rs2618479, and rs2248932, while a recent study looking specifically at BLK in a multi-racial group (Guthridge et al. *Am J Hum Genet*. 2014;94(4):586–598) found the top Asian variant was rs1478901. Looking at the linkage disequilibrium between these variants, we see r^2<0.77 and D'>0.97 between all variants other than rs2248932, which has r^2<0.48 and D'<0.71. These studies likely have identified the same effect, but rs2248932 identified in the Han Chinese study may represent an independent effect in this population.

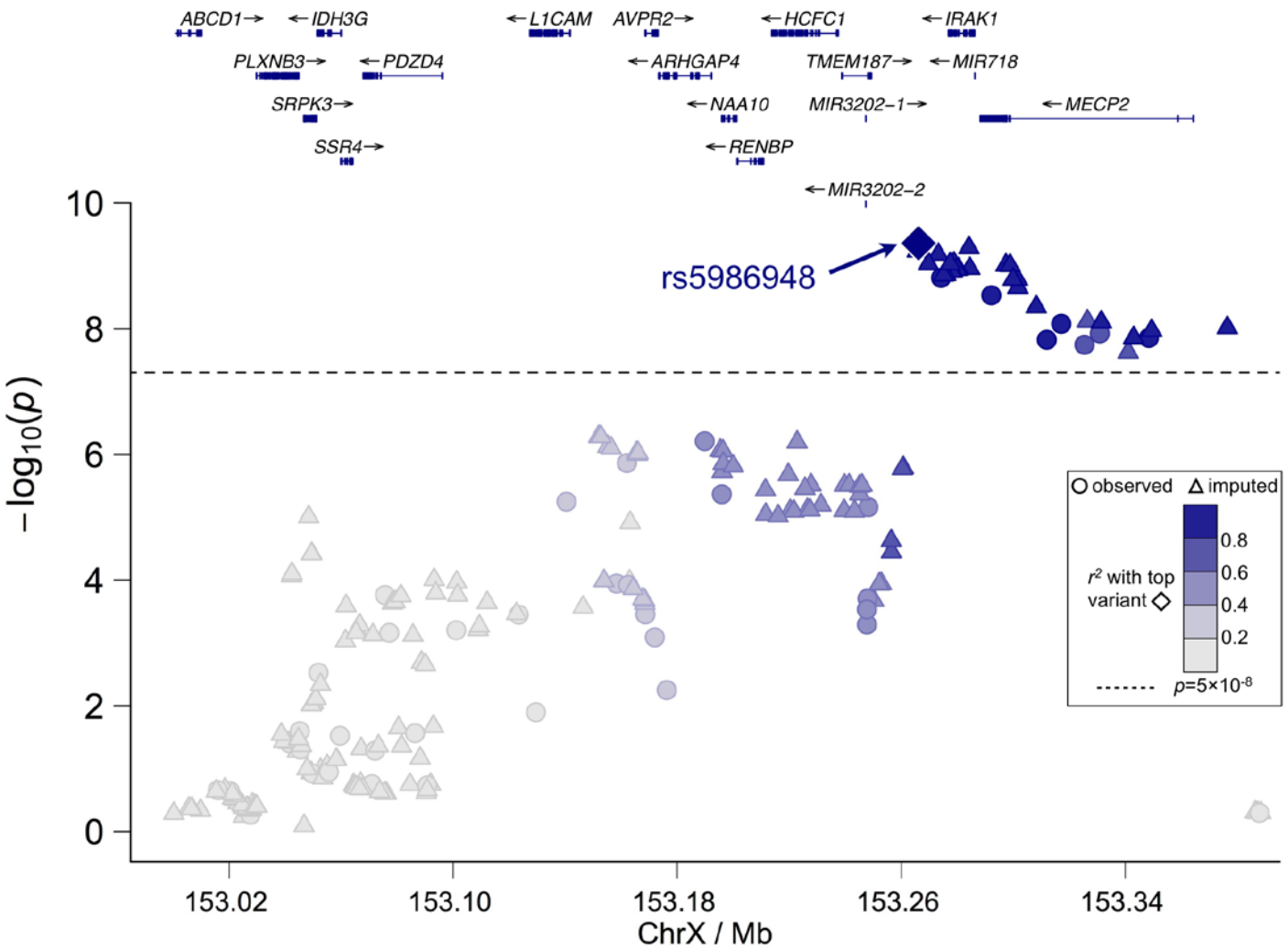

Supplementary Figure 11: Zoom plot of the single locus analysis with SLE in the region of *IRAK1-MECP2.* In the region of IRAK1-MECP2 after imputation, only a single independent effect was identified in the stepwise model lead by rs5986948 (blue diamond). A previous study evaluating this region in a multi-racial SLE population (Kaufman et al. Ann Rheum Dis, 2013 72(3) 437-444) identified the top variant as rs1059702, which was among the top associations in this current Korean study. The variant rs1059702 is in strong linkage disequilibrium with rs5986948 (r^2=0.92; D'=1.0) indicating they likely represent the same effect.

For the following Supplementary Tables, please see the accompanying Excel spreadsheet:

Please note: Missing genotypes have been imputed into this dataset if they were not called in the GWAS dataset.

Supplementary Table 6: Summary of the single locus analysis with SLE after imputation in the region of *STAT4*

Supplementary Table 7: Summary of the single locus analysis with SLE after imputation in the region of *IKZF1*

Supplementary Table 8: Summary of the single locus analysis with SLE after imputation in the region of *TNFAIP3*

Supplementary Table 9: Summary of the single locus analysis with SLE after imputation in the region of *TNFSF4*

Supplementary Table 10: Summary of the single locus analysis with SLE after imputation in the region of *HIP1*

Supplementary Table 11: Summary of the single locus analysis with SLE after imputation in the region of *IRF5*

Supplementary Table 12: Summary of the single locus analysis with SLE after imputation in the region of *ETS1*

Supplementary Table 13: Summary of the single locus analysis with SLE after imputation in the region of *BLK*

Supplementary Table 14: Summary of the single locus analysis with SLE after imputation in the region of *WDFY4*

Supplementary Table 15: Summary of the single locus analysis with SLE in the region of *IRAK1-MECP2*

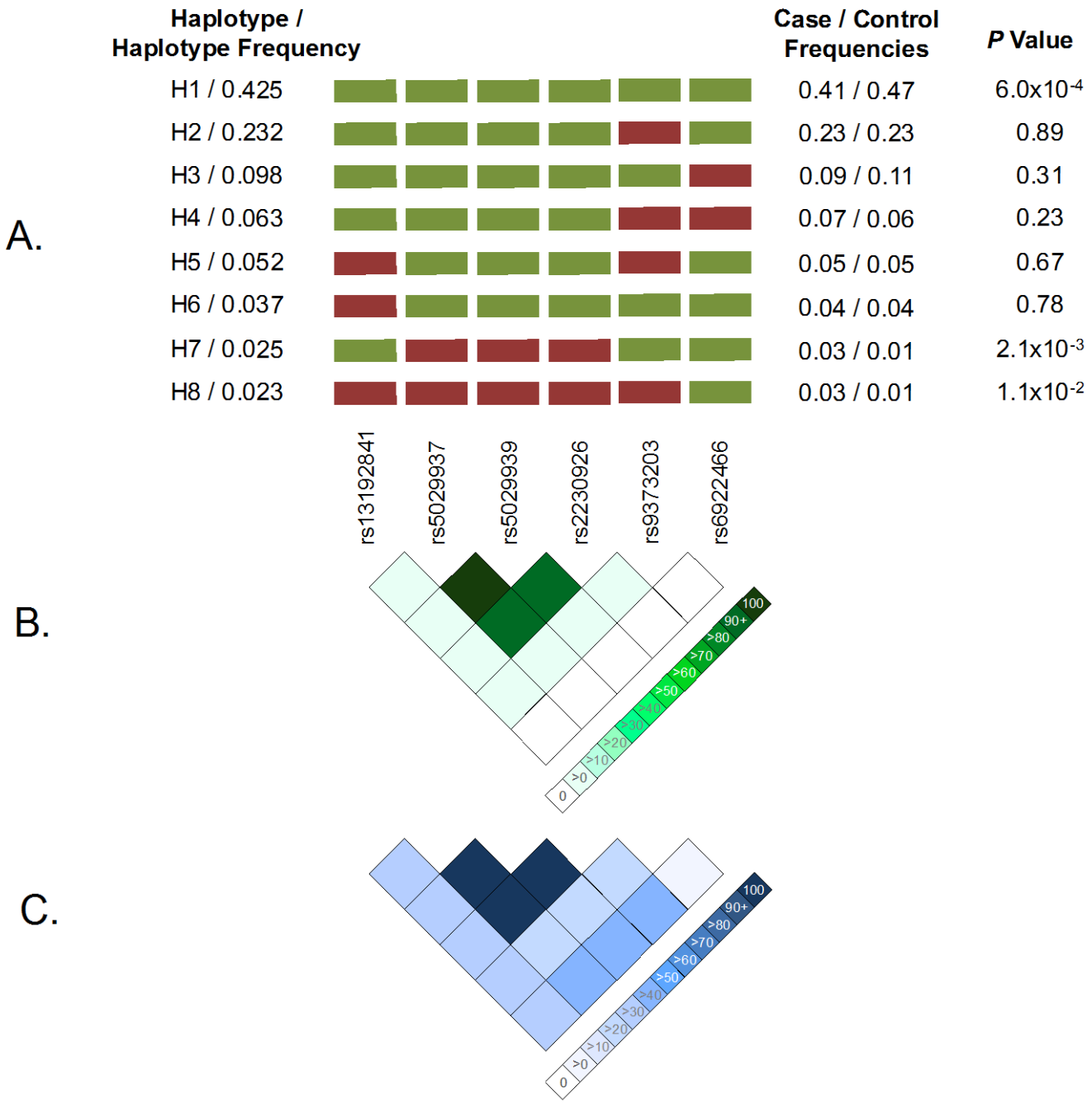

Supplementary Figure 12: Haplotype and linkage disequilibrium disequlibrium structure in the region of *TNFAIP3* in Koreans. To better understand the relationship of the variants that have been described as associated within this region, we evaluated the haplotype structure and linkage disequilibrium between each locus. Each haplotype with a frequency >2% is given, with the major alleles in green and the minor alleles in red (A). The pair-wise linkage disequilibrium between each variant is given r^2 (B) and D' (C), with the magnitude according to the legend presented to the right of each plot.

A.

Haplotype / Haplotype Frequency	Case / Control Frequencies	*P* Value
H1 / 0.415	0.41 / 0.43	0.30
H2 / 0.196	0.22 / 0.15	9.7×10^{-7}
H3 / 0.142	0.13 / 0.18	2.0×10^{-4}
H4 / 0.065	0.06 / 0.07	0.61
H5 / 0.064	0.06 / 0.06	0.95
H6 / 0.058	0.06 / 0.06	0.64
H7 / 0.020	0.02 / 0.02	0.99
H8 / 0.011	0.01 / 0.01	0.82

B.

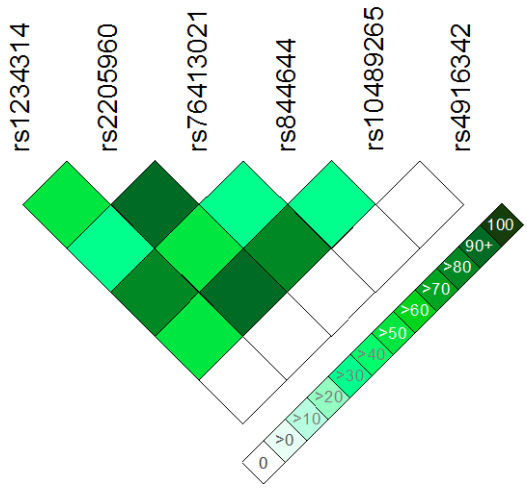

C.

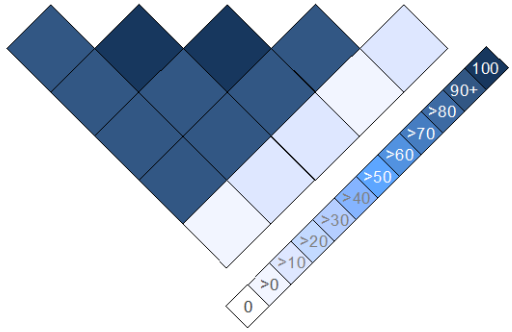

Supplementary Figure 13: Haplotype and linkage disequilibrium structure in the region of *TNFSF4* in Koreans. To better understand the relationship of the variants that have been described as associated within this region, we evaluated the haplotype structure and linkage disequilibrium between each locus. Each haplotype with a frequency >2% is given with the major alleles in green and the minor alleles in red (A). The pair-wise linkage disequilibrium between each variant is given r^2 (B) and D' (C), with the magnitude according to the legend presented to the right of each plot.

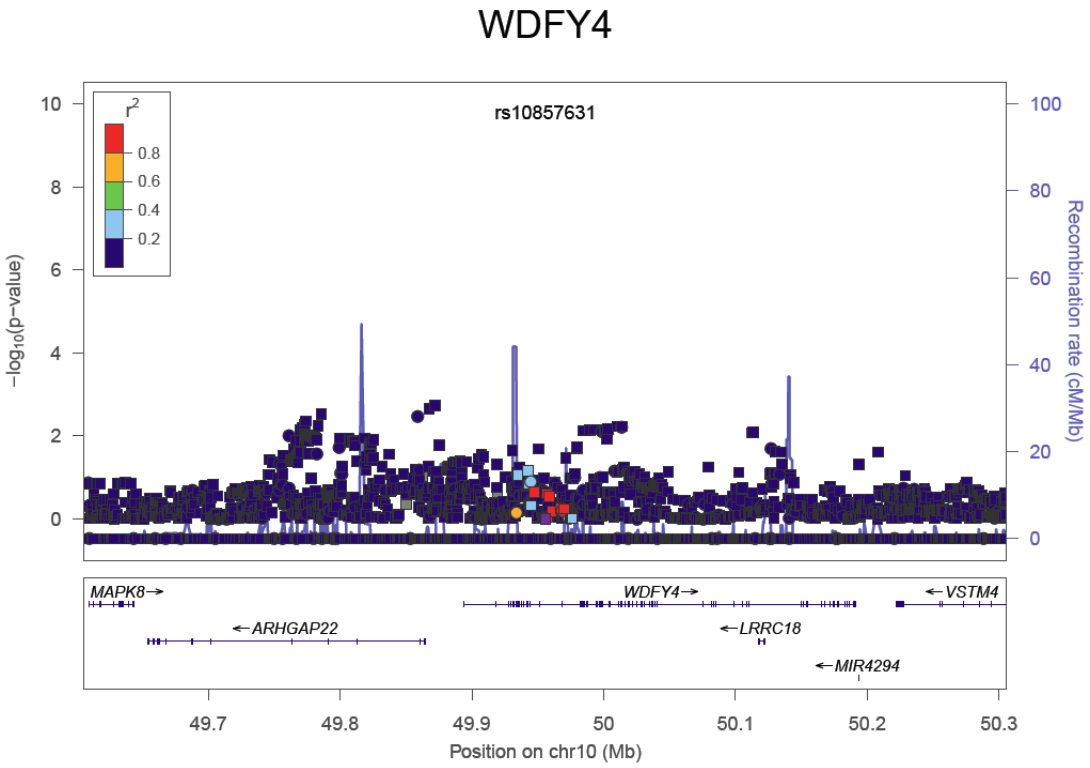

Supplementary Figure 14: Stepwise regression analysis of the *WDFY4* region adjusting for rs7097397 and rs1913517. Our stepwise model in the region of *WDFY4* showed two independent effects that were accounted for by rs7097397 and rs1913517.

A.

Haplotype / Haplotype Frequency	Case / Control Frequencies	*P* Value
H1 / 0.491	0.469 / 0.537	2.0×10^{-4}
H2 / 0.132	0.141 / 0.113	0.0219
H3 / 0.132	0.126 / 0.145	0.1267
H4 / 0.086	0.088 / 0.082	0.5515
H5 / 0.038	0.043 / 0.030	0.0732
H6 / 0.035	0.038 / 0.029	0.1621
H7 / 0.023	0.027 / 0.015	0.0226
H8 / 0.023	0.027 / 0.015	0.0417

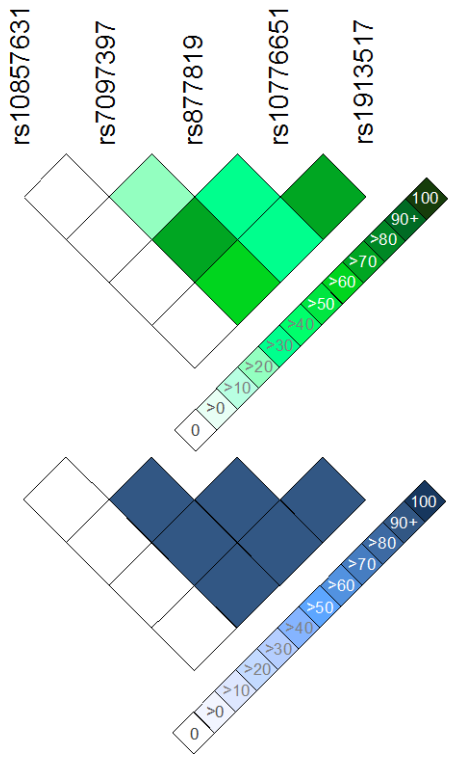

Supplementary Figure 15: Haplotype and linkage disequilibrium of the *WDFY4* region. To gain a clearer understanding as to why rs877819 was not associated in this study, we performed a haplotype analysis. (a) The haplotype structure of the variants of interest with frequency >2%. The major alleles are represented by red squares while the minor alleles are in green for each variant listed below the figure. The current study found association with rs7097397 as the most significantly associated variant with SLE, which had also been reported by Zhao et al. 2012[23]. Moreover, we also identified rs1913517, previously reported by Han et al. 2009[9]. Looking at the risk haplotypes, H2 and H7 are risk haplotypes with the protective allele (the major allele) for rs877819, while only H8 has all variants in their risk form. The structure of the linkage disequilibrium (LD) measured by both r^2 (b) and D' (c) are given for the relevant variants with the intensity of the LD increasing with the color scheme given on the right. Although there is relatively strong D' between rs7097397, rs877819, rs10776651, and rs1913517, the pair-wise r^2 between rs877819 and the rest of the variants is relatively low. Thus, these data suggest that the risk alleles of rs7097397 and rs1913517 are in strong D' with the major allele of rs877819, which is the non-risk allele according to Zhao et al. 2012[23]. In addition, it is clear that rs10857631 is an independent risk allele with no LD with the other variants of interest in this region.

Supplementary Table 16: Summary of suggestive associations ($P < 2x10^{-6}$ to $P>5x10^{-8}$) from the single locus analysis of genotyped variant from the GWAS array with SLE

Marker	Chr	Pos	Upstream Gene	Downstream Gene	Within Gene	Allele A/B	MAF Case / Ctrl	P	Model	OR (95% CI)
rs4572645	2	133187785	-	-	GPR39	G/A	0.37 / 0.34	1.25E-06	Rec	1.57 (1.31-1.89)
rs6819946	4	10702156	None within 500 kb.	15.77 kb from CLNK	-	C/T	0.40 / 0.46	1.25E-06	Add	0.80 (0.73-0.87)
rs9291444	4	10713674	None within 500 kb.	27.288 kb from CLNK	-	T/C	0.40 / 0.45	1.82E-06	Add	0.80 (0.73-0.88)
rs4368598	4	10714656	None within 500 kb.	28.27 kb from CLNK	-	C/T	0.14 / 0.18	1.43E-06	Add	0.72 (0.63-0.82)
rs2074660	7	73922613	-	-	GTF2IRD1	A/G	0.40 / 0.45	1.14E-06	Add	0.79 (0.72-0.87)
rs2267828	7	73926112	-	-	GTF2IRD1	T/C	0.40 / 0.45	7.02E-07	Add	0.79 (0.72-0.87)
rs10901656	10	128386150	207.872 kb from DOCK1	176.14 kb from C10orf90	-	C/T	0.27 / 0.23	6.91E-07	Dom	1.39 (1.22-1.58)
rs739389	11	65157094	-	-	FRMD8	C/T	0.43 / 0.47	6.92E-07	Dom	0.71 (0.61-0.81)
rs10791824	11	65559266	-	-	OVOL1	A/G	0.40 / 0.46	1.19E-07	Dom	0.69 (0.61-0.79)
rs1048257	14	105404384	-	-	AHNAK2	A/G	0.34 / 0.39	1.67E-06	Add	0.79 (0.72-0.87)
rs11623422	14	105407031	-	-	AHNAK2	A/G	0.34 / 0.39	9.81E-07	Add	0.79 (0.71-0.87)
rs11851053	14	105407208	-	-	AHNAK2	T/C	0.34 / 0.39	1.25E-06	Add	0.79 (0.72-0.87)
rs4465542	14	105407798	-	-	AHNAK2	T/C	0.34 / 0.39	1.28E-06	Add	0.79 (0.72-0.87)

Supplementary Table 17: Summary of suggestive associations ($P < 5x10^{-5}$ to $P>5x10^{-8}$) from the single locus analysis with SLE previously established with disease.

Marker	Chr	Pos	Upstream Gene	Downstream Gene	Within Gene	Allele A/B	MAF Case / Ctrl	P	Model	OR (95% CI)
rs1801274	1	161479745	-	-	FCGR2A	T/C	0.29 / 0.24	7.08E-06	Dom	1.35 (1.18-1.53)
rs6699818	1	161673508	3.253 kb from FCRLA	18.466 kb from RPL31P11	-	C/T	0.11 / 0.08	1.88E-05	Dom	1.43 (1.21-1.69)
rs13385731	2	33701890	-	-	RASGRP3	T/C	0.10 / 0.13	1.47E-06	Add	0.69 (0.59-0.80)
rs2367735	2	33702679	-	-	RASGRP3	G/T	0.44 / 0.40	3.57E-05	Add	1.22 (1.11-1.33)
rs12494314	3	119122820	-	-	ARHGAP31	T/C	0.28 / 0.32	4.75E-05	Add	0.81 (0.73-0.90)
rs3732421	3	119150089	-	-	TMEM39A	A/G	0.27 / 0.31	4.57E-05	Add	0.81 (0.73-0.90)
rs10236415	7	35444548	227.721 kb from HERPUD2	28.462 kb from LOC401324	-	C/A	0.20 / 0.16	1.56E-05	Dom	1.35 (1.18-1.55)
rs10262622	7	35523030	149.239 kb from HERPUD2	106.944 kb from LOC401324	-	T/C	0.21 / 0.17	2.87E-05	Dom	1.33 (1.17-1.53)
rs7965575	12	129271459	6.279 kb from SLC15A4	78.999 kb from TMEM132C	-	T/C	0.31 / 0.37	3.72E-06	Add	0.79 (0.72-0.87)
rs1059312	12	129278864	-	-	SLC15A4	T/C	0.52 / 0.46	1.99E-06	Add	1.25 (1.14-1.37)
rs9738216	12	129281788	-	-	SLC15A4	T/C	0.51 / 0.46	2.80E-06	Add	1.25 (1.14-1.36)
rs11644034	16	85972612	347.424 kb from LOC146513	16.401 kb from IRF8	-	G/A	0.06 / 0.09	1.31E-05	Add	0.66 (0.55-0.80)
rs10521318	16	86011337	308.699 kb from LOC146513	55.126 kb from IRF8	-	G/A	0.07 / 0.10	3.68E-06	Add	0.67 (0.56-0.79)
rs2077579	11	118619047	-	-	DDX6	T/G	0.12 / 0.15	1.85E-05	Add	0.73 (0.64-0.85)
rs4938573	11	118741842	12.632 kb from CXCR5	79.87 kb from DDX6	-	T/C	0.10 / 0.14	1.89E-05	Add	0.72 (0.62-0.84)
rs7892586	X	12833100	-	-	PRPS2	A/C	0.26 / 0.31	4.93E-05	Add	0.74 (0.61-0.90)
rs7062536	X	12839152	-	-	PRPS2	A/G	0.28 / 0.32	1.22E-05	Add	0.69 (0.57-0.84)

Supplementary Table 18: Functional effects of established SLE risk loci.

Gene	SNP	Functional Effect	Subphenotype Associations	Gene Function
TNFAIP3	rs14314165, rs200820567 (ref. 1)	The TT to A deletion (TT>A) for rs14314165 and rs200820567, respectivly, results in a decreased amount of TNFAIP3 transcript and A20 protein (ref. 1). In a follow up paper, the TT>A was shown to abolish a SAT1B site responsible for the complex chromatin interaction of this region looping back to the promoter (ref. 2). This element acts as an enhancer as shown by luciferase assays (ref. 2).	The SNP rs5029939 (a perfect proxy for rs14314165 and rs200820567) is associated with nephritis, malar rash, photosensitivity, arthritis, oral ulcers, serositis, hematologic, and immunologic manifestations of SLE (ref. 3).	TNFAIP3 encodes the protein A20 that is a negative regulator of NF-κB responses (ref. 4). Cell-type specific conditional deletion in B cells and dendritic cells yielded lupus-like phenotypes in mice with autoantibody production, Ig deposition in the kidneys, and nephritis. (ref. 4)
TNFSF4	rs2205960, rs1234314 (ref. 5)	The T allele of the SNP rs2205960 forms an NF-κBp65 binding motif with increased affinity as compared to the G allele (ref. 5). This variant has been reported to be an eQTL for the TNFSF4 transcript in normal twins (ref. 6).	rs2205960 is associated with autoantibody production and lymphopenia (ref. 5).	TNFSF4 encodes the protein OX40 ligand (OX40L) that is secreted by antigen presenting cells and acts as a strong co-stimulatory signal for naive and memory $CD4^+$ T cells (ref. 5). These $CD4^+$ T cells are then induced to the T follicular helper cell state. In pediatric and adult lupus, myeloid antigen presenting cells were found to express OX40L, and the circulating frequency of these cells was correlated with disease activity and circulating T follicular helper cell numbers (ref. 7).
IRF5	rs2004640, Exon 6 in-frame deletion, rs10954213 (refs. 8 and 9); rs4728142, rs12534421 (ref. 10)	Multiple functional effects have been found within the IRF5 risk locus. Graham et al. found that a promoter variant, rs2004640, alters expression of the IRF5 transcript. They also show that the variant rs10954213 leads to a longer 3' poly-A sequence for IRF5, thereby prolonging the half-life of the transcript (refs 8 and 9). The exon 6 deletion resides in a region known to influence the stability and function of the protein. In Kottyan et al., the authors assessed >3000 variants in the IRF5 locus for association with SLE (ref. 10). Using a Bayesian method, the group of SNPs that were highly correlated was reduced and the most likely candidates were evaluated for functionality. The SNP rs4728142 was found to alter the binding site for ZBTB3, leading to altered expression of IRF5 transcript (ref. 10).	The risk haplotype in IRF5 is associated with anti-dsDNA and anti-Ro autoantibodies (ref. 11).	IRF5 is an transcription factor that is involved in TLR7 responses leading to the expression of proinflammatory molecules, such as IL12B, IL6, and interferon-γ (ref. 12). IRF5 also has been implicated in a wide-range of other pathways important in SLE pathophysiology: macrophage polarization, B cell differentiatoin into plasma cells, IgG class switching, and apoptosis (ref. 12). All these pathways have been implicated in SLE, and it is likley that IRF5 risk is attributed to many, if not all, of these functions. (ref. 12)
BLK	rs922483 and rs1382568 (tri-allelic; ref. 13)	The risk allele T for rs922483 results in a decrease in promoter activity and selection of an alternative transcriptional start site for the BLK locus (ref. 13). This allele alters the expression of BLK most significantly. The risk allele C for rs1382568 also alters expression of BLK (ref. 13). Pro-B and Pre-B cells lines seem to be the most affected by these alterations in transcription of BLK, while immature B, mature B, and Jurkat cell lines seem to be unaffected (ref. 13).	Healthy subjects were found to have an increased amount of anti-dsDNA autoantibodies in a BLK risk-allele dependent manner (rs2736340; ref. 14).	BLK is a non-receptor Src family tyrosine kinase and is downregulated upon BCR stimulation. Mice defficent in BLK produce antinuclear autoantibodies and show an increase in B1a cell numbers (Wu et al. 2015). BLK risk genotypes affect numbers of B1-like cells in the periphery of healthy carriers, and B1-like cells have been shown to accumulate in the kidney biopsy tissue of SLE patients (ref. 14).
IRAK1-MECP2	rs1059702 (change in amino acid sequence, S196F, in IRAK1; ref. 15); rs1734787 (ref. 16)	The risk allele for rs1059702 results in an amino acid substitution, S196F, which has been shown to alter NF-κB activity (ref. 15). This variant also results in a decrease in MECP2 mRNA levels, but IRAK1 mRNA levels are not influenced by this variant (ref. 15). The halotype tagged by rs1734787 has been shown to influence expression of 128 genes (104 upregulated and 24 downregulated in B cells of lupus patients (ref. 16). Interestingly, 13 of the 104 are interferon-related transcripts (ref. 16)		In mice, the IRAK1 gene has been shown to influence IgM and IgG autoantibodies, lymphocytic activation, and renal disease (ref. 17). MECP2 incorporates DNA methylation and histone deacetylation to silence gene expression, which has been suggested to play a role in SLE (ref. 15).
IKZF1	rs491701 (ref. 18)	For the SNP associated with SLE, rs491701, the T allele has been shown to bind more weakly to IKZF1 promoter sequences using ChIP-seq data (ref. 19). Since this variant influences expression of IKZF1, which is a transcription factor, rs491701 also has many *trans* effects resulting in altered expression of complement genes (CLEC10A, C1QB) and type I interferon genes (CLEC4C, IFI6, HERC5, IFIT1, TNFRSF21, MX1), many of which have been implicated in SLE pathogenesis previously (ref. 19).	The SNP rs491701 is assocated with malar rash and renal nephritis (ref. 20).	The gene IKZF1 encodes the protein Ikaros that is a lymphoid restricted transcription factor for genes involved in lymphocyte differentiation (ref. 21). Ikaros in essential for DC terminal differentiation (ref. 21). The protein also regulates the expression ot T-bet, the master regulator of T helper 1 cell commitment, leading to a decrease in the production of Interferon-γ (ref. 21).
HIP1	rs1167796 (ref. 18)	A GWAS study by Han et al. found the SNP rs1167796 as the peak association in the region, which encompasses multiple genes (ref. 18). To date, no published work has identified the definitive causal variant in this region, but rs1167796 is reported by Westra et al. as an eQTL for HIP1 (ref. 19).		
ETS1	rs1128334, rs6590330 (ref. 22).	The risk allele, A, of rs1128334 results in a significant reduction in ETS1 transcript in Asians (ref. 23). The risk allele for rs6590330 results in a increase in binding of pSTAT1 from B cell lysates and a decrease in ETS1 expression (ref. 22).	The SNP rs1128334 is assocated with age at lupus diagnosis of less than 20 years old (ref. 20).	ETS1 is a transcription factor that works to regulate B cell differentiation into plasma cells. Deletion of ETS1 in mice results in the accumulation of autoreactive plasma cells, the production of autoantibodies, and an autoimune phenotype similar to lupus (ref. 24).

References for Supplementary Table 18.

1. Adrianto I, Wen F, Templeton A, Wiley G, King JB, Lessard CJ, Bates JS, Hu Y, Kelly JA, Kaufman KM, Guthridge JM, Alarcón-Riquelme ME, BIOLUPUS and GENLES Networks, Anaya J-M, Bae S-C, Bang S-Y, Boackle SA, Brown EE, Petri MA, Gallant C, Ramsey-Goldman R, Reveille JD, Vilá LM, Criswell LA, Edberg JC, Freedman BI, Gregersen PK, Gilkeson GS, Jacob CO, James JA, Kamen DL, Kimberly RP, Martín J, Merrill JT, Niewold TB, Park S-Y, Pons-Estel BA, Scofield RH, Stevens AM, Tsao BP, Vyse TJ, Langefeld CD, Harley JB, Moser KL, Webb CF, Humphrey MB, Montgomery CG, Gaffney PM. Association of a functional variant downstream of TNFAIP3 with systemic lupus erythematosus. Nat Genet. 2011 Mar;43(3):253–8. PMCID: PMC3103780

2. Wang S, Wen F, Wiley GB, Kinter MT, Gaffney PM. An enhancer element harboring variants associated with systemic lupus erythematosus engages the TNFAIP3 promoter to influence A20 expression. PLoS Genet. 2013;9(9):e1003750. PMCID: PMC3764111

3. Bates JS, Lessard CJ, Leon JM, Nguyen T, Battiest LJ, Rodgers J, Kaufman KM, James JA, Gilkeson GS, Kelly JA, Humphrey MB, Harley JB, Gray-Mcguire C, Moser KL, Gaffney PM. Meta-analysis and imputation identifies a 109 kb risk haplotype spanning TNFAIP3 associated with lupus nephritis and hematologic manifestations. Genes Immun. 2009 Jul;10(5):470–7. PMCID: PMC2714405

4. Ma A, Malynn BA. A20: linking a complex regulator of ubiquitylation to immunity and human disease. Nat Rev Immunol. 2012 Nov;12(11):774–85.

5. Manku H, Langefeld CD, Guerra SG, Malik TH, Alarcon-Riquelme M, Anaya J-M, Bae S-C, Boackle SA, Brown EE, Criswell LA, Freedman BI, Gaffney PM, Gregersen PA, Guthridge JM, Han S-H, Harley JB, Jacob CO, James JA, Kamen DL, Kaufman KM, Kelly JA, Martin J, Merrill JT, Moser KL, Niewold TB, Park S-Y, Pons-Estel BA, Sawalha AH, Scofield RH, Shen N, Stevens AM, Sun C, Gilkeson GS, Edberg JC, Kimberly RP, Nath SK, Tsao BP, Vyse TJ. Trans-ancestral studies fine map the SLE-susceptibility locus TNFSF4. PLoS Genet. 2013;9(7):e1003554. PMCID: PMC3715547

6. Grundberg E, Small KS, Hedman AK, Nica AC, Buil A, Keildson S, Bell JT, Yang T-P, Meduri E, Barrett A, Nisbett J, Sekowska M, Wilk A, Shin S-Y, Glass D, Travers M, Min JL, Ring S, Ho K, Thorleifsson G, Kong A, Thorsteindottir U, Ainali C, Dimas AS, Hassanali N, Ingle C, Knowles D, Krestyaninova M, Lowe CE, Di Meglio P, Montgomery SB, Parts L, Potter S, Surdulescu G, Tsaprouni L, Tsoka S, Bataille V, Durbin R, Nestle FO, O'Rahilly S, Soranzo N, Lindgren CM, Zondervan KT, Ahmadi KR, Schadt EE, Stefansson K, Smith GD, McCarthy MI, Deloukas P, Dermitzakis ET, et al. Mapping cis- and trans-regulatory effects across multiple tissues in twins. Nat Genet. Nature Publishing Group; 2012 Oct;44(10):1084–9. PMCID: PMC3784328

7. Jacquemin C, Schmitt N, Contin-Bordes C, Liu Y, Narayanan P, Seneschal J, Maurouard T, Dougall D, Davizon ES, Dumortier H, Douchet I, Raffray L, Richez C, Lazaro E, Duffau P, Truchetet M-E, Khoryati L, Mercié P, Couzi L, Merville P, Schaeverbeke T, Viallard J-F, Pellegrin J-L, Moreau J-F, Muller S, Zurawski S, Coffman RL, Pascual V, Ueno H, Blanco

P. OX40 Ligand Contributes to Human Lupus Pathogenesis by Promoting T Follicular Helper Response. Immunity. Elsevier; 2015 Jun 16;42(6):1159–70. PMCID: PMC4570857

8. Graham RR, Cotsapas C, Davies L, Hackett R, Lessard CJ, Leon JM, Burtt NP, Guiducci C, Parkin M, Gates C, Plenge RM, Behrens TW, Wither JE, Rioux JD, Fortin PR, Graham DC, Wong AK, Vyse TJ, Daly MJ, Altshuler D, Moser KL, Gaffney PM. Genetic variants near TNFAIP3 on 6q23 are associated with systemic lupus erythematosus. Nat Genet. 2008 Sep;40(9):1059–61. PMCID: PMC2772171

9. Graham RR, Kyogoku C, Kyogoku C, Sigurdsson S, Vlasova IA, Vlasova IA, Davies LRL, Davies LRL, Baechler EC, Plenge RM, Plenge RM, Koeuth T, Koeuth T, Ortmann WA, Hom G, Bauer JW, Bauer JW, Gillett C, Gillett C, Burtt N, Burtt N, Cunninghame Graham DS, Onofrio R, Onofrio R, Petri M, Gunnarsson I, Svenungsson E, Ronnblom L, Nordmark G, Gregersen PK, Moser K, Moser K, Gaffney PM, Criswell LA, Vyse TJ, Syvanen A-C, Bohjanen PR, Bohjanen PR, Daly MJ, Behrens TW, Altshuler D. Three functional variants of IFN regulatory factor 5 (IRF5) define risk and protective haplotypes for human lupus. Proceedings of the National Academy of Sciences. 2007 Apr 17;104(16):6758–63. PMCID: PMC1847749

10. Kottyan LC, Zoller EE, Bene J, Lu X, Kelly JA, Rupert AM, Lessard CJ, Vaughn SE, Marion M, Weirauch MT, Namjou B, Adler A, Rasmussen A, Glenn S, Montgomery CG, Hirschfield GM, Xie G, Coltescu C, Amos C, Li H, Ice JA, Nath SK, Mariette X, Bowman S, UK Primary Sjögren's Syndrome Registry, Rischmueller M, Lester S, Brun JG, Gøransson LG, Harboe E, Omdal R, Cunninghame Graham DS, Vyse T, Miceli-Richard C, Brennan MT, Lessard JA, Wahren-Herlenius M, Kvarnström M, Illei GG, Witte T, Jonsson R, Eriksson P, Nordmark G, Ng W-F, Anaya J-M, Rhodus NL, Segal BM, Merrill JT, James JA, Guthridge JM, et al. The IRF5-TNPO3 association with systemic lupus erythematosus has two components that other autoimmune disorders variably share. Human Molecular Genetics. 2015 Jan 15;24(2):582–96. PMCID: PMC4275071

11. Niewold TB, Kelly JA, Kariuki SN, Franek BS, Kumar AA, Kaufman KM, Thomas K, Walker D, Kamp S, Frost JM, Wong AK, Merrill JT, Alarcón-Riquelme ME, Tikly M, Ramsey-Goldman R, Reveille JD, Petri MA, Edberg JC, Kimberly RP, Alarcón GS, Kamen DL, Gilkeson GS, Vyse TJ, James JA, Gaffney PM, Moser KL, Crow MK, Harley JB. IRF5 haplotypes demonstrate diverse serological associations which predict serum interferon alpha activity and explain the majority of the genetic association with systemic lupus erythematosus. Ann Rheum Dis. 2012 Mar;71(3):463–8. PMCID: PMC3307526

12. 1. Lazzari E, Jefferies CA. IRF5-mediated signaling and implications for SLE. Clin Immunol. 2014 Aug;153(2):343–52.

13. Guthridge JM, Lu R, Sun H, Sun C, Wiley GB, Dominguez N, Macwana SR, Lessard CJ, Kim-Howard X, Cobb BL, Kaufman KM, Kelly JA, Langefeld CD, Adler AJ, Harley ITW, Merrill JT, Gilkeson GS, Kamen DL, Niewold TB, Brown EE, Edberg JC, Petri MA, Ramsey-Goldman R, Reveille JD, Vilá LM, Kimberly RP, Freedman BI, Stevens AM, Boackle SA, Criswell LA, Vyse TJ, Behrens TW, Jacob CO, Alarcón-Riquelme ME, Sivils KL, Choi J, Joo YB, Bang S-Y, Lee H-S, Bae S-C, Shen N, Qian X, Tsao BP, Scofield RH, Harley JB,

Webb CF, Wakeland EK, James JA, Nath SK, Graham RR, et al. Two Functional Lupus-Associated BLK Promoter Variants Control Cell-Type- and Developmental-Stage-Specific Transcription. Am J Hum Genet. 2014 Apr 3;94(4):586–98.

14. Wu Y-Y, Georg I, Díaz-Barreiro A, Varela N, Lauwerys B, Kumar R, Bagavant H, Castillo-Martín M, Salem El F, Marañón C, Alarcón-Riquelme ME. Concordance of increased B1 cell subset and lupus phenotypes in mice and humans is dependent on BLK expression levels. J Immunol. 2015 Jun 15;194(12):5692–702. PMCID: PMC4458437

15. Kaufman KM, Zhao J, Kelly JA, Hughes T, Adler A, Sanchez E, Ojwang JO, Langefeld CD, Ziegler JT, Williams AH, Comeau ME, Marion MC, Glenn SB, Cantor RM, Grossman JM, Hahn BH, Song YW, Yu C-Y, James JA, Guthridge JM, Brown EE, Alarcón GS, Kimberly RP, Edberg JC, Ramsey-Goldman R, Petri MA, Reveille JD, Vilá LM, Anaya J-M, Boackle SA, Stevens AM, Freedman BI, Criswell LA, Pons-Estel BA, Argentine Collaborative Group, Lee J-H, Lee J-S, Chang D-M, Scofield RHA, Gilkeson GS, Merrill JT, Niewold TB, Vyse TJ, Bae S-C, Alarcón-Riquelme ME, BIOLUPUS Network, Jacob CO, Moser Sivils K, Gaffney PM, Harley JB, et al. Fine mapping of Xq28: both MECP2 and IRAK1 contribute to risk for systemic lupus erythematosus in multiple ancestral groups. Ann Rheum Dis. 2013 Mar;72(3):437–44. PMCID: PMC3567234

16. Webb R, Wren JD, Jeffries M, Kelly JA, Kaufman KM, Tang Y, Frank MB, Merrill J, Kimberly RP, Edberg JC, Ramsey-Goldman R, Petri M, Reveille JD, Alarcón GS, Vilá LM, Alarcón-Riquelme ME, James JA, Vyse TJ, Moser KL, Gaffney PM, Gilkeson GS, Harley JB, Sawalha AH. Variants within MECP2, a key transcription regulator, are associated with increased susceptibility to lupus and differential gene expression in patients with systemic lupus erythematosus. 2009 Apr;60(4):1076–84. PMCID: PMC2734382

17. Jacob CO, Zhu J, Armstrong DL, Yan M, Han J, Zhou XJ, Thomas JA, Reiff A, Myones BL, Ojwang JO, Kaufman KM, Klein-Gitelman M, McCurdy D, Wagner-Weiner L, Silverman E, Ziegler J, Kelly JA, Merrill JT, Harley JB, Ramsey-Goldman R, Vilá LM, Bae S-C, Vyse TJ, Gilkeson GS, Gaffney PM, Moser KL, Langefeld CD, Zidovetzki R, Mohan C. Identification of IRAK1 as a risk gene with critical role in the pathogenesis of systemic lupus erythematosus. Proc Natl Acad Sci USA. National Acad Sciences; 2009 Apr 14;106(15):6256–61. PMCID: PMC2669395

18. Han J-W, Zheng H-F, Cui Y, Sun L-D, Ye D-Q, Hu Z, Xu J-H, Cai Z-M, Huang W, Zhao G-P, Xie H-F, Fang H, Lu Q-J, Xu J-H, Li X-P, Pan Y-F, Deng D-Q, Zeng F-Q, Ye Z-Z, Zhang X-Y, Wang Q-W, Hao F, Ma L, Zuo X-B, Zhou F-S, Du W-H, Cheng Y-L, Yang J-Q, Shen S-K, Li J, Sheng Y-J, Zuo X-X, Zhu W-F, Gao F, Zhang P-L, Guo Q, Li B, Gao M, Xiao F-L, Quan C, Zhang C, Zhang Z, Zhu K-J, Li Y, Hu D-Y, Lu W-S, Huang J-L, Liu S-X, Li H, Ren Y-Q, et al. Genome-wide association study in a Chinese Han population identifies nine new susceptibility loci for systemic lupus erythematosus. Nat Genet. 2009 Nov 1;41(11):1234–7.

19. Westra H-J, Peters MJ, Esko T, Yaghootkar H, Schurmann C, Kettunen J, Christiansen MW, Fairfax BP, Schramm K, Powell JE, Zhernakova A, Zhernakova DV, Veldink JH, van den Berg LH, Karjalainen J, Withoff S, Uitterlinden AG, Hofman A, Rivadeneira F, 't Hoen PAC, Reinmaa E, Fischer K, Nelis M, Milani L, Melzer D, Ferrucci L, Singleton AB,

Hernandez DG, Nalls MA, Homuth G, Nauck M, Radke D, Völker U, Perola M, Salomaa V, Brody J, Suchy-Dicey A, Gharib SA, Enquobahrie DA, Lumley T, Montgomery GW, Makino S, Prokisch H, Herder C, Roden M, Grallert H, Meitinger T, Strauch K, Li Y, Jansen RC, et al. Systematic identification of trans eQTLs as putative drivers of known disease associations. Nat Genet. 2013 Sep 8.

20. He C-F, Liu Y-S, Cheng Y-L, Gao J-P, Pan T-M, Han J-W, Quan C, Sun L-D, Zheng H-F, Zuo X-B, Xu S-X, Sheng Y-J, Yao S, Hu W-L, Li Y, Yu Z-Y, Yin X-Y, Zhang X-J, Cui Y, Yang S. TNIP1, SLC15A4, ETS1, RasGRP3 and IKZF1 are associated with clinical features of systemic lupus erythematosus in a Chinese Han population. Lupus. SAGE Publications; 2010 Sep;19(10):1181–6.

21. Hu S-J, Wen L-L, Hu X, Yin X-Y, Cui Y, Yang S, Zhang X-J. IKZF1: a critical role in the pathogenesis of systemic lupus erythematosus? Mod Rheumatol. 2013 Mar;23(2):205–9.

22. Lu X, Zoller EE, Weirauch MT, Wu Z, Namjou B, Williams AH, Ziegler JT, Comeau ME, Marion MC, Glenn SB, Adler A, Shen N, Nath SK, Stevens AM, Freedman BI, Tsao BP, Jacob CO, Kamen DL, Brown EE, Gilkeson GS, Alarcón GS, Reveille JD, Anaya J-M, James JA, Sivils KL, Criswell LA, Vilá LM, Alarcón-Riquelme ME, Petri M, Scofield RH, Kimberly RP, Ramsey-Goldman R, Joo YB, Choi J, Bae S-C, Boackle SA, Graham DC, Vyse TJ, Guthridge JM, Gaffney PM, Langefeld CD, Kelly JA, Greis KD, Kaufman KM, Harley JB, Kottyan LC. Lupus Risk Variant Increases pSTAT1 Binding and Decreases ETS1 Expression. Am J Hum Genet. 2015 May 7;96(5):731–9. PMCID: PMC4570281

23. Yang W, Shen N, Ye D-Q, Liu Q, Zhang Y, Qian X-X, Hirankarn N, Ying D, Pan H-F, Mok CC, Chan TM, Wong RWS, Lee KW, Mok MY, Wong SN, Leung AMH, Li X-P, Avihingsanon Y, Wong C-M, Lee TL, Ho MHK, Lee PPW, Chang YK, Li PH, Li R-J, Zhang L, Wong WHS, Ng IOL, Lau CS, Sham PC, Lau YL, Asian Lupus Genetics Consortium. Genome-wide association study in Asian populations identifies variants in ETS1 and WDFY4 associated with systemic lupus erythematosus. PLoS Genet. 2010 Feb;6(2):e1000841. PMCID: PMC2820522

24. Mayeux J, Skaug B, Luo W, Russell LM, John S, Saelee P, Abbasi H, Li Q-Z, Garrett-Sinha LA, Satterthwaite AB. Genetic Interaction between Lyn, Ets1, and Btk in the Control of Antibody Levels. J Immunol. American Association of Immunologists; 2015 Sep 1;195(5):1955–63. PMCID: PMC4546901